



Published in final edited form as:

*Circ Res.* 2023 April 28; 132(9): e116–e133. doi:10.1161/CIRCRESAHA.122.321858.

## Enhanced Ca<sup>2+</sup>-Dependent SK-Channel Gating and Membrane Trafficking in Human Atrial Fibrillation

Jordi Heijman, PhD<sup>1,2,\*</sup>, Xiaobo Zhou, MD<sup>3,4,\*</sup>, Stefano Morotti, PhD<sup>5</sup>, Cristina E. Molina, PhD<sup>6</sup>, Issam H. Abu-Taha, PhD<sup>1</sup>, Marcel Tekook, PhD<sup>1</sup>, Thomas Jespersen, PhD<sup>7</sup>, Yiqiao Zhang<sup>1</sup>, Shokoufeh Dobrev, PhD<sup>1</sup>, Hendrik Milting, PhD<sup>8</sup>, Jan Gummert, MD<sup>8</sup>, Matthias Karck, MD<sup>9</sup>, Markus Kamler, MD<sup>10</sup>, Ali El-Armouche, MD<sup>11</sup>, Arnela Saljic, PhD<sup>1,7</sup>, Eleonora Grandi, PhD<sup>5</sup>, Stanley Nattel, MD<sup>1,12,13,14</sup>, Dobromir Dobrev, MD<sup>1,12,15</sup>

<sup>1</sup>Institute of Pharmacology, West German Heart and Vascular Center, Faculty of Medicine, University Duisburg-Essen, Essen, Germany

<sup>2</sup>Department of Cardiology, Cardiovascular Research Institute Maastricht, Faculty of Health, Medicine, and Life Sciences, Maastricht University, Maastricht, The Netherlands

<sup>3</sup>First Department of Medicine, Medical Faculty Mannheim, Heidelberg University, Mannheim, Germany and DZHK (German Center for Cardiovascular Research), partner site Heidelberg/Mannheim, Mannheim, Germany

<sup>4</sup>Key Laboratory of Medical Electrophysiology, Ministry of Education and Medical Electrophysiological Key Laboratory of Sichuan Province, Collaborative Innovation Center for Prevention of Cardiovascular Diseases, Institute of Cardiovascular Research, Southwest Medical University, Luzhou, Sichuan, China

<sup>5</sup>Department of Pharmacology, University of California, Davis, CA, USA

<sup>6</sup>Institute of Experimental Cardiovascular Research, University Medical Center Hamburg-Eppendorf and DZHK (German Center for Cardiovascular Research), partner site Hamburg/Kiel/Lübeck, Hamburg, Germany

<sup>7</sup>Department of Biomedical Sciences, Faculty of Health and Medical Sciences, University of Copenhagen, Copenhagen, Denmark.

<sup>8</sup>Erich and Hanna Klessmann Institute, Heart and Diabetes Center NRW, University Hospital of the Ruhr-University Bochum, Bad Oeynhausen, Germany.

<sup>9</sup>Department of Cardiac Surgery, Heidelberg University Hospital, Heidelberg, Germany

<sup>10</sup>Department of Thoracic and Cardiovascular Surgery, West German Heart and Vascular Center Essen, University Hospital Essen, Germany

<sup>11</sup>Institute of Pharmacology, Dresden University of Technology, Germany

**Corresponding Author:** Dobromir Dobrev, MD, Institute of Pharmacology, Hufelandstr 55, D-45122 Essen, Germany, Phone: +49-201-733-3477, Fax: +49-201-723-5593, dobromir.dobrev@uk-essen.de.

\*Shared first authorship

Disclosures

The authors have no relevant conflicts of interest to disclose.

<sup>12</sup>Department of Medicine, Montreal Heart Institute and Université de Montréal

<sup>13</sup>Department of Pharmacology and Therapeutics, McGill University Montreal, Canada

<sup>14</sup>IHU LIRYC and Fondation Bordeaux Université, Bordeaux, France

<sup>15</sup>Department of Molecular Physiology & Biophysics, Baylor College of Medicine, Houston, TX, USA

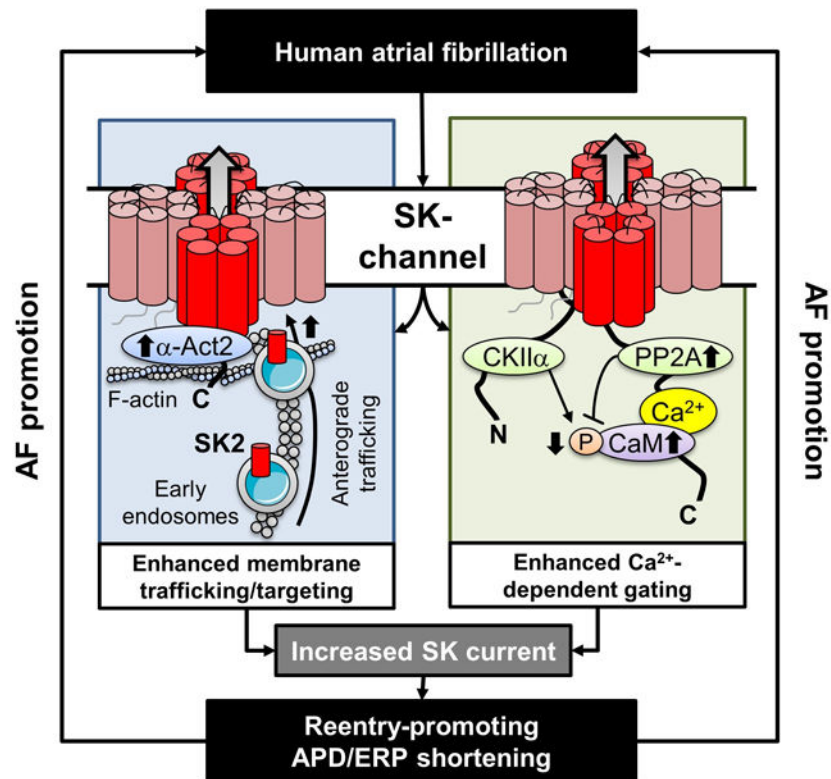
## Abstract

**Background:** Small-conductance  $\text{Ca}^{2+}$ -activated  $\text{K}^+$  (SK)-channel inhibitors have antiarrhythmic effects in animal models of atrial fibrillation (AF), presenting a potential novel antiarrhythmic option. However, the regulation of SK-channels in human atrial cardiomyocytes and its modification in AF-patients are poorly understood and were the object of this study.

**Methods and Results:** Apamin-sensitive SK-channel current ( $I_{\text{SK}}$ ) and action potentials (APs) were recorded in human right-atrial cardiomyocytes from control sinus-rhythm (Ctl) or long-term persistent (chronic) AF (cAF) patients.  $I_{\text{SK}}$  was significantly higher and apamin caused larger AP-prolongation in cAF- vs. Ctl-cardiomyocytes. Sensitivity analyses in an *in silico* human atrial cardiomyocyte model identified  $I_{\text{K1}}$  and  $I_{\text{SK}}$  as major regulators of repolarization. Increased  $I_{\text{SK}}$  in cAF was not associated with increases in mRNA/protein levels of SK-channel subunits in either right- or left-atrial tissue homogenates or right-atrial cardiomyocytes, but the abundance of SK2 at the sarcolemma was larger in cAF vs. Ctl in both tissue-slices and cardiomyocytes. Latrunculin-A and primaquine (anterograde and retrograde protein-trafficking inhibitors) eliminated the differences in SK2 membrane levels and  $I_{\text{SK}}$  between Ctl- and cAF-cardiomyocytes. In addition, the phosphatase-inhibitor okadaic acid reduced  $I_{\text{SK}}$  amplitude and abolished the difference between Ctl- and cAF-cardiomyocytes, indicating that reduced calmodulin-Thr80 phosphorylation due to increased protein phosphatase-2A levels in the SK-channel complex likely contribute to the greater  $I_{\text{SK}}$  in cAF-cardiomyocytes. Finally, rapid electrical activation (5-Hz, 10-minutes) of Ctl-cardiomyocytes promoted SK2 membrane-localization, increased  $I_{\text{SK}}$  and reduced AP-duration, effects greatly attenuated by apamin. Latrunculin-A or primaquine prevented the 5-Hz-induced  $I_{\text{SK}}$ -upregulation.

**Conclusions:**  $I_{\text{SK}}$  is upregulated in cAF-patients due to enhanced channel function, mediated by phosphatase-2A-dependent calmodulin-Thr80 dephosphorylation and tachycardia-dependent enhanced trafficking and targeting of SK-channel subunits to the sarcolemma. The observed AF-associated increases in  $I_{\text{SK}}$ , which promote reentry-stabilizing APD-shortening, suggest an important role for SK-channels in AF auto-promotion, and provide a rationale for pursuing the antiarrhythmic effects of SK-channel inhibition in humans.

## Graphical Abstract



## Keywords

Arrhythmias; Calcium cycling/excitation-contraction coupling; Computational biology; atrial fibrillation; ion channels/membrane transport; atrial fibrillation; calcium-activated K<sup>+</sup>-channels; calmodulin Thr80-phosphorylation; channel trafficking and targeting; action potential duration; remodeling; tachycardia

## Introduction

Atrial fibrillation (AF) is a major healthcare problem, contributing to increased morbidity and mortality worldwide.<sup>1</sup> Accumulating evidence indicates that rhythm-control therapy may improve outcomes in AF-patients, particularly when the treatment is initiated early.<sup>2,3</sup> Despite the widespread use of AF-ablation, antiarrhythmic drug (AAD) therapy continues to be important for rhythm-control strategies, both as initial therapy and when ablation fails or is not advisable. However, current AADs have limited efficacy and non-negligible risks, particularly drug-induced proarrhythmia.<sup>4</sup> Atrial-selective AADs have been proposed as safer, more effective alternatives,<sup>5</sup> but conceptual, practical and regulatory challenges have hindered the development of new AADs for AF.<sup>4</sup>

Small-conductance Ca<sup>2+</sup>-activated K<sup>+</sup> (SK or K<sub>Ca2.X</sub>)-channels, encoded by *KCNKI-3*, have been suggested as promising targets for pharmacological rhythm-control therapy.<sup>6</sup> SK-channel expression and current ( $I_{SK}$ ) are upregulated in several animal models of AF, including dogs with 7-days of electrically-maintained AF<sup>7</sup> and rabbits with 3-h intermittent

atrial-burst pacing.<sup>8</sup> SK-channel inhibitors prolong atrial repolarization, promote AF-termination in rats,<sup>9</sup> dogs,<sup>7</sup> goats<sup>10</sup> horses,<sup>11</sup> and pigs,<sup>12,13</sup> and reduce the likelihood of subsequent AF-reinduction.<sup>13</sup> Moreover, SK-channel inhibition in pigs can successfully terminate more persistent forms of AF that are resistant to cardioversion by vernakalant,<sup>13</sup> an AAD clinically approved in Europe and several other jurisdictions, suggesting a robust antiarrhythmic efficacy in large animals with remodeled atria.

In humans, common genetic variants in *KCNN2* and *KCNN3* have been associated with AF in genome-wide association studies<sup>14</sup> and first-in-human studies with SK-channel inhibitors have recently been initiated,<sup>15</sup> making SK-channels one of the few novel AAD targets in active clinical development.<sup>4</sup> However, the direction of molecular remodeling of SK-channels in AF-patients remains controversial. The AF-associated genetic variant rs13376333 in *KCNN3* has been linked to increased *KCNN3* mRNA-expression in human atria,<sup>16</sup> whereas several studies have reported a downregulation of SK-channel subunit mRNA expression in AF-patients (Table S1).<sup>17–20</sup> Moreover, results depend on the anatomic region of interest<sup>7</sup> and presence of specific systemic modulators.<sup>19</sup>

In the brain  $I_{SK}$  is regulated by modulation of  $Ca^{2+}$ -dependent gating through dynamic phosphorylation of SK-channel-associated calmodulin at Thr80.<sup>21</sup> The open probability of single SK-channels is increased in dogs with atrial tachycardia remodeling,<sup>7</sup> pointing to upregulated  $Ca^{2+}$ -dependent gating of individual SK-channels. Calmodulin is not only essential for gating, but is also required for channel assembly, trafficking and targeting.<sup>22</sup> SK2-channel trafficking is  $Ca^{2+}$ -dependent in HEK293 cells, suggesting that a rise in  $Ca^{2+}$ , e.g., during atrial tachyarrhythmias may increase the membrane targeting of SK2 channels.<sup>23</sup> In agreement, the magnitude of  $I_{SK}$  can be modulated rapidly by atrial tachypacing via increased SK-channel trafficking in rabbits.<sup>8</sup> Thus, mRNA levels are only poor indicators of functional SK-channel remodeling and  $I_{SK}$  appears to be very sensitive to rapid rhythms like AF, with  $Ca^{2+}$  regulating both upstream channel trafficking including membrane targeting and individual channel gating.

The complex SK-channel regulation by numerous signaling pathways and stressors make functional characterization of SK-channel remodeling in human atrial cardiomyocytes essential, but data on  $I_{SK}$  in patients with or without AF are scarce.  $I_{SK}$  or repolarization-prolongation by SK-channel inhibition are increased in atrial cardiomyocytes from AF-patients compared to sinus rhythm control (Ctl) patients in most studies,<sup>20,24,25</sup> but decreased<sup>17,26</sup> in some (Table S2). Whether calmodulin-dependent regulation of  $Ca^{2+}$ -dependent SK-channel gating, dynamic SK-channel trafficking and tachycardia-dependent  $I_{SK}$  upregulation are operative in human atrial cardiomyocytes, and whether and how they are affected by human AF, are unknown and were the object of this study.

We performed a comprehensive assessment of the molecular and functional remodeling of SK-channels in right-atrial (RA) and left-atrial (LA) samples from Ctl and long-standing persistent (chronic) AF (cAF) patients to test the hypothesis that increased function of individual SK-channels and augmented subunit trafficking and targeting to the plasmalemma contribute to an increased  $I_{SK}$  in cAF-patients. Our results reveal complex regulation of  $I_{SK}$  in AF-patients, attributable to changes in phosphorylation and trafficking/targeting, that

sheds insight into the molecular control of  $I_{SK}$  in AF and its potential as an antiarrhythmic target.

## Methods

### Data Availability.

The original data that support the findings of this study are available from the corresponding author upon reasonable request..

A detailed description of all methods is provided in the online-only Data Supplement and the Major Resources Table. Key aspects are summarized below

**Human atrial samples**—Patients (>18 years) undergoing open-heart surgery without a history of AF (Ctl group) or with a clinical diagnosis of persistent (chronic) AF (cAF group) were included and RA- and/or LA-appendages were obtained (Tables S3–S10). In addition, dedicated patient cohorts were included with a history of heart failure (HF) with reduced (< 35%) left-ventricular ejection-fraction with or without cAF (HFrEF-SR and HFrEF-cAF groups, respectively), as well as Ctl- and cAF-patients for whom paired RA- and LA-samples were available (Tables S11–S12). All samples were collected just prior to atrial cannulation for extracorporeal circulatory bypass, and were immediately used for cardiomyocyte isolation and subsequent patch-clamp recordings or immunocytochemistry, or were flash-frozen in liquid nitrogen for biochemical experiments. In total, samples from 301 patients were studied (182 Ctl, 119 cAF). Experimental protocols were approved by ethical review boards of University Hospital Essen (#12–5268-BO), Medical Faculty Mannheim, University of Heidelberg (2011–216N-MA) and Medical Faculty, Ruhr-Universität Bochum (No. AZ 21/2013), and were conducted in accordance with the Declaration of Helsinki. Each patient provided written informed consent.

**Cardiomyocyte isolation and patch-clamp recordings**—Cardiomyocytes were isolated from RA-samples using previously described enzymatic-digestion protocols.<sup>27</sup> Membrane-currents were recorded at room temperature in the whole-cell ruptured-patch voltage-clamp configuration in the absence or presence of the SK-channel inhibitor apamin (100-nmol/L).  $I_{SK}$  was defined as the apamin-sensitive current and corrected for membrane capacitance (expressed as pA/pF), whereas intermediate-conductance (SK4) and big-conductance  $Ca^{2+}$ -activated  $K^+$  (BKCa) currents were recorded as Tram-34 (100-nmol/L) and iberiotoxin (300-nmol/L)-sensitive currents, respectively, as previously described.<sup>28,29</sup> APs were elicited in current-clamp configuration using a 2-ms 1-nA stimulus applied every 5000-ms in the presence of a –40-pA holding current. All patch-clamp experiments were performed in the presence of 500-nmol/L free intracellular  $Ca^{2+}$ , unless indicated otherwise.

**Quantitative polymerase chain reaction**—Total RNA was isolated from RA whole-tissue homogenates and RA cardiomyocytes from Ctl and cAF patients and reverse-transcription or digital polymerase chain reactions were performed as described in the online-only Data Supplement<sup>30</sup> using primers based on published sequences (see Major Resources Table).

**Co-immunoprecipitation and immunoblot**—Proteins were isolated from atrial whole-tissue homogenates or human atrial cardiomyocytes according to standard protocols.<sup>31,32</sup> Co-immunoprecipitation and immunoblot were employed to determine protein levels as previously described.<sup>31,33</sup> Antibodies are listed in the Major Resources Table.

**Immunocytochemistry**—Isolated human RA-cardiomyocytes or cryosections from RA- or LA-tissue samples were incubated overnight at 4°C with primary antibodies against SK1, SK2, SK3 or  $\alpha$ -actinin2. Wheat-germ agglutinin was used for membrane staining in cryosections. Samples were subsequently incubated with AlexaFluor® 488/568/633 secondary antibodies and imaged using a confocal microscope or Keyence BZ-X800E. Antibodies are listed in the Major Resources Table.

**Computational modeling**—We integrated a new SK-channel formulation in the Ctl and cAF versions of our previous human atrial cardiomyocyte model.<sup>34–36</sup> Parameters of the updated model were optimized to reproduce recent experimental data on APD and Ca<sup>2+</sup>-transient properties under a wide range of experimental conditions (Computational Modeling Section in the online-only Data Supplement). The model was employed to assess the impact of SK-channel inhibition on APD and resting membrane potential. A population-of-models approach<sup>37</sup> was used to simulate inter-individual heterogeneity in ionic currents and determine the relative contribution of I<sub>SK</sub> to human atrial electrophysiology. The model code is freely available on the authors' website (see Major Resources Table).

**Statistics**—Results are presented as scatter-plots and mean±standard deviation for normally-distributed data or median and interquartile ranges for non-normally-distributed data. Representative images and traces were chosen based on image quality and agreement with the average difference between groups. A complete overview of all Western blots is provided as supplemental material. Normality was tested using D'Agostino&Pearson omnibus testing in Prism-7 (GraphPad Software, San Diego, CA).

For biochemical experiments and clinical parameters, for which each patient contributed a single data-point, unpaired two-tailed Student's t-tests with Welch's correction were employed to compare means of normally-distributed continuous data, since heterogeneous variances are common. Non-normally-distributed continuous data or data for which normality could not be assessed were compared using Mann-Whitney tests. Categorical data were analyzed using Chi-squared tests.

For patch-clamp recordings and immunocytochemistry, in which each patient may contribute multiple data points, data were defined (1) by the individual patient ID and (2) the ID of the cardiomyocyte within each patient. Sample-sizes are given as n/N, where n=cardiomyocytes and N=patients. Multilevel mixed-effect models were employed to compare groups, as previously described.<sup>38</sup> The random effect within the model was the intercept to account for non-independent measurements in multiple cells from individual patients. Multilevel models were implemented in RStudio (Boston, MA) using lme4 with P-values derived using the Kenward-Roger approximation. Non-normally distributed data were log-transformed and P-values for multiple comparisons within a single panel were Bonferroni-corrected.



## Results

### Patient characteristics

Patient characteristics are provided in Tables S3–S12. Overall, cAF-patients were significantly older and more often had valve disease as the primary indication for their cardiac surgery (Table S3), in line with previous studies.<sup>17,39</sup> As expected, cAF-patients also had significantly larger left-atrial diameters and more often used digitalis (Table S3). Diuretics were more commonly prescribed to cAF- compared to Ctl-patients (Table S3).

### Larger Ca<sup>2+</sup>-activated K<sup>+</sup>-currents in cAF-patients result in a significantly greater APD-prolongation upon SK-channel inhibition

We recorded K<sup>+</sup>-currents in Ctl and cAF RA-cardiomyocytes and used the highly-selective SK-channel inhibitor apamin to quantify the specific contribution of I<sub>SK</sub>.<sup>40</sup> Apamin (100-nmol/L) slightly decreased total membrane current in Ctl-cardiomyocytes (Figure 1A) and had a significantly larger effect in cAF-cardiomyocytes (Figure 1B). The apamin-sensitive current was largely voltage-independent (Figure 1C), not detectable in the absence of intracellular Ca<sup>2+</sup> (Figure S1A–C), and showed the expected dependence on intracellular [Ca<sup>2+</sup>] (Figure S1D), consistent with characteristics of I<sub>SK</sub>. Both inward and outward components of I<sub>SK</sub> were significantly larger in cAF-cardiomyocytes compared to Ctl-cardiomyocytes; Figure 1C,D). Although the primary subunits of SK4 and BKCa-channels are widely expressed<sup>41</sup> and could be detected at the protein level in human RA whole-tissue homogenates, there were no significant differences in protein levels between Ctl- and cAF-patients (Figure S2A). Moreover, the SK4-channel blocker Tram34 (100-nmol/L) and the BKCa-channel blocker iberiotoxin (300-nmol/L) did not affect total membrane current in human RA-cardiomyocytes (Figure S2B). We therefore focused on apamin-sensitive I<sub>SK</sub>.

To assess whether I<sub>SK</sub>-upregulation affected APs, we performed current-clamp recordings in the absence or presence of apamin in Ctl and cAF RA-cardiomyocytes (Figure 1E). Apamin (100-nmol/L) did not affect resting membrane potential or AP amplitude (Figure S3A,B), but significantly prolonged APD at 50% and 90% repolarization (APD<sub>50</sub> and APD<sub>90</sub>, respectively) in both Ctl- and cAF-cardiomyocytes (Figure S3C). The apamin-induced APD prolongation was significantly larger in cAF (APD<sub>50</sub>: 23.9±13.9%, APD<sub>90</sub>: 39.2±26.6%; n=8/7) compared to Ctl (APD<sub>50</sub>: 3.4±2.5%, APD<sub>90</sub>: 11.0±6.9%; n=8/5; Figure 1F), consistent with the greater I<sub>SK</sub> in cAF.

We then developed a novel *in silico* human atrial cardiomyocyte model parameterization (Figures S4–S9) to validate the contribution of I<sub>SK</sub> to atrial repolarization. The model incorporated known AF-related electrical and Ca<sup>2+</sup>-handling remodeling elements and accurately reproduced experimentally observed AP-properties, including the extent of APD prolongation by I<sub>SK</sub>-inhibition (Figure S7). The model also predicted that during regular 1-Hz pacing with cAF-associated Ca<sup>2+</sup> transients, APD was shorter and I<sub>SK</sub> was larger in cAF cells, with I<sub>SK</sub>-inhibition producing a much stronger relative prolongation of APD<sub>90</sub> in cAF compared to Ctl at all pacing rates from 0.1 to 4 Hz (Figure S10).

To assess the relative contribution of I<sub>SK</sub> to APD and RMP in Ctl and cAF, a population of 1000 models with variations in maximal conductances of all major ion channels was

generated (Figure 2A). In addition, the affinity of  $I_{SK}$  for intracellular  $[Ca^{2+}]$  ( $K_{D,SK}$ ) was varied since previous studies have reported an increased affinity in cAF- vs. Ctl-patients.<sup>20</sup> Model-based sensitivity analyses identified a major contribution of  $I_{SK}$  conductance to  $APD_{50}$  and  $APD_{90}$ , with a switch from basal inward-rectifier  $K^+$  current ( $I_{K1}$  and constitutively-active acetylcholine-activated inward-rectifier  $K^+$  current,  $I_{K,ACH,c}$ ) to  $I_{SK}$  dominance for controlling  $APD_{90}$  in cAF (Figure 2B), pointing to a potential role for  $I_{SK}$  in determining the vulnerability to reentry. By contrast,  $K_{D,SK}$  only had a modest impact on APD, which was confirmed by simulations reproducing the larger, experimentally observed, 100 nmol/L difference in  $[Ca^{2+}]$  affinity between Ctl and cAF cardiomyocytes<sup>20</sup> (Figure S11).  $I_{SK}$  also had little effect on resting membrane potential, which was primarily determined by  $I_{K1}/I_{K,ACH,c}$  (Figure 2B).

### Reduced calmodulin phosphorylation and increased SK-channel membrane trafficking underlie the increased $I_{SK}$ in cAF-patients

The mRNA-levels of *KCNN1* and *KCNN2* (encoding SK1 and SK2, respectively) were similar between RA whole-tissue homogenates of Ctl- and cAF-patients, whereas mRNA-levels of *KCNN3* (encoding SK3) were significantly increased in cAF (Figure S12). At the protein level (see validation of the SK2 antibody in Figure S13A), there were no significant differences between Ctl- and cAF-patients for any of the three subunits in either RA (Figure S13B) or LA whole-tissue homogenates (Figure S13C). Since endothelial cells and fibroblasts also express SK channels, we also assessed mRNA and protein levels of SK-channel subunits in human RA-cardiomyocytes. The SK2 mRNA levels were decreased in cAF- vs. Ctl-patients (Figure S14–S15), consistent with previous studies (Table S1), but protein levels of SK-subunits were not significantly different between Ctl- and cAF-cardiomyocytes (Figure 2C). Since previous work identified  $Ca^{2+}$ -dependent upregulation of SK-channel gating and trafficking in expression systems and animal models,<sup>8,22,23</sup> we hypothesized that these mechanisms may underlie the larger  $I_{SK}$  in cAF-cardiomyocytes in the absence of differences in total protein levels.

We investigated the subcellular localization of SK-channel subunits in RA- and LA-tissue slices, employing co-staining with wheat-germ agglutinin to delineate the sarcolemma (Figures S16–S18). The relative membrane/cytosol fluorescence intensity of SK3 was not significantly different between Ctl- and cAF-cardiomyocytes in either RA- or LA-samples, whereas the SK2 membrane/cytosol ratio was larger in both RA- and LA-samples of cAF- compared to Ctl-patients (Figure 3), suggesting a potential role for increased SK2-membrane levels in the increased  $I_{SK}$  in cAF-patients. Similar changes were seen in isolated RA-cardiomyocytes; the membrane/cytosol ratio of SK2 (but not SK1 or SK3) was significantly increased in cAF- compared to Ctl-cardiomyocytes (Figure 4A,C; Figure S19). To assess potential underlying mechanisms, we evaluated trafficking changes with the use of the actin-depolymerizing agent latrunculin-A (1- $\mu$ mol/L for 2-hours) and the early (recycling) endosome inhibitor primaquine (120- $\mu$ mol/L for 4-hours), which modulate anterograde and retrograde protein trafficking, respectively,<sup>42,43</sup> both SK2- and SK3-levels were significantly reduced in cAF cells, reaching levels comparable to Ctl-cardiomyocytes (Figure 4B,C). Consistent with these data, there was no significant difference in  $I_{SK}$ -amplitude between Ctl- and cAF-cardiomyocytes in the presence of either latrunculin-A



or primaquine (Figure 5A,B). Thus, upregulated trafficking-mediated SK2-channel subunit targeting to the plasma membrane may contribute to the larger  $I_{SK}$  in cAF-patients.

SK channels are organized in macromolecular complexes including calmodulin, casein kinase type-II (CKII) and protein phosphatase type-2A (PP2A), along with trafficking- and targeting-related proteins (Figure S20; Figure 6A).<sup>6,21</sup> Phosphorylation of calmodulin at Thr80 by CKII decreases  $Ca^{2+}$ -sensitivity, reducing  $I_{SK}$ , whereas PP2A-dependent dephosphorylation of calmodulin-Thr80 increases  $I_{SK}$ .<sup>21</sup> Selective inhibition of PP2A with okadaic acid (10-nmol/L for 1-hour) significantly reduced  $I_{SK}$  in cAF-cardiomyocytes, suggesting that increased PP2A contributes to enhanced  $I_{SK}$  in cAF. (Figure 5C,D). We then investigated whether altered PP2A and CKII $\alpha$  expression contributes to calmodulin phosphorylation and thus to the increased  $I_{SK}$  in cAF.

To exclude confounding effects of non-cardiomyocyte compartments, we noted a significant increase in total calmodulin expression in cAF-cardiomyocytes (Figure 6B,C), which in itself may contribute to the greater  $I_{SK}$ . Moreover, relative Thr80-phosphorylation of calmodulin was significantly decreased (Figure 6B,C). The lower Thr80-phosphorylation of calmodulin is likely due to increased protein levels of the PP2A catalytic subunit (PP2Ac) in atrial cardiomyocytes of cAF-patients (Figure 6D), consistent with our prior observations in whole-atrial tissue.<sup>31</sup> There was also a non-significant increase in total calmodulin protein levels and a decrease in calmodulin phosphorylation in RA whole-tissue homogenates, resulting in a tendency ( $P=0.085$ ) towards reduced relative calmodulin Thr80-phosphorylation levels in cAF (Figure S21A,B). Total CKII $\alpha$  protein levels were not significantly different between Ctl and cAF (Figure S21C). The lack of statistically-significant differences was likely due to contamination by non-cardiomyocyte cells. Importantly, we identified similar changes in calmodulin expression, Thr80-phosphorylation and PP2Ac expression in LA homogenates from cAF- vs. Ctl-patients (Figure S22), suggesting comparable remodeling of SK-channel regulation in both atria. Finally, we assessed PP2Ac levels in the SK2-channel macromolecular complex using immunoprecipitation of RA-tissue samples (Figure 6E): PP2Ac levels associated with the SK2 complex were significantly increased in RA of cAF- vs. Ctl-patients (Figure 6F). Thus, enhanced PP2A-mediated Thr80-dephosphorylation of SK-channel-associated calmodulin likely contributes to the greater  $I_{SK}$  in cAF-patients.

Previous work has shown that forward trafficking and recycling of SK2 from early endosomes and SK2 membrane insertion/retention are also  $Ca^{2+}$  dependent and rely on calmodulin and the SK2-interacting protein  $\alpha$ -actinin2.<sup>23,44</sup> Based on the increased SK2 membrane levels in cAF-patients (Figures 3,4), we assessed whether a stronger interaction between  $\alpha$ -actinin2 and SK2 as an index of increased SK2 membrane insertion/retention occurs in cAF. Although total  $\alpha$ -actinin2 protein levels were not significantly different between Ctl- and cAF-groups in RA and LA whole-tissue homogenates and RA-cardiomyocytes (Figure S23), the SK2-associated  $\alpha$ -actinin2 levels were larger in immunoprecipitates from cAF vs. Ctl RA-tissue homogenates (Figure 6F). Furthermore, RA-cardiomyocytes from cAF-patients incubated in membrane-permeable BAPTA-AM (25- $\mu$ mol/L for 5-hours) revealed strongly reduced SK2-membrane levels (Figure 6G), pointing

to contribution of a  $\text{Ca}^{2+}$ -dependent,  $\alpha$ -actinin2-mediated trafficking mechanism to the increased SK2-membrane levels in cAF.

### AF-mimicking in vitro tachypacing increases $I_{\text{SK}}$ by enhancing membrane trafficking

Atrial tachycardia causes rapid cellular  $\text{Ca}^{2+}$ -loading<sup>45</sup> and increases SK-channel trafficking in rabbit pulmonary vein cardiomyocytes within minutes.<sup>8</sup> Similarly, a high atrial rate during AF would be expected to contribute to the  $\text{Ca}^{2+}$ -dependent upregulation of SK-channel activity in cAF-patients. To test this hypothesis, we compared  $I_{\text{SK}}$  at baseline with  $I_{\text{SK}}$  in RA Ctl-cardiomyocytes subjected to 10-minutes of AP-like depolarizing voltage-clamp pulses at 5-Hz (Figure 7A).

The 10-minutes of 5-Hz activation significantly increased  $I_{\text{SK}}$  in RA Ctl-cardiomyocytes compared to baseline (Figure 7B), reaching levels similar to those of cAF-cardiomyocytes after 5-Hz activation (Figure 7B). Since repeated measurements of apamin-sensitive  $I_{\text{SK}}$  are not possible due to the slow washout of apamin, the time course of total membrane current ( $I_{\text{M}}$ ) before and after 10-minute 5-Hz activation was evaluated as a proxy for  $I_{\text{SK}}$  to study reversibility of tachypacing-induced SK-channel remodeling. In RA-cardiomyocytes from Ctl-patients, 10 minutes of 5-Hz activation increased  $I_{\text{M}}$  at +80 mV by  $9.50 \pm 1.41$  pA/pF ( $n=5/5$ ; Figure S24A). In comparison, in RA Ctl-cardiomyocytes the difference in mean apamin-sensitive  $I_{\text{SK}}$  at +80 mV between baseline and 10-minute 5-Hz activation was 6.33 pA/pF (Figure 7B), suggesting that the majority of the pacing-induced increase in  $I_{\text{M}}$  is due to  $I_{\text{SK}}$ . During a subsequent 5-min follow-up period  $I_{\text{M}}$  decayed from  $26.65 \pm 1.10$  to  $24.58 \pm 0.72$  pA/pF ( $P=5.49 \times 10^{-4}$ ; Figure S24A), resulting in a decay rate of 0.46 (0.32–0.48) pA/pF  $\text{min}^{-1}$  and a predicted linear time to baseline of 25 minutes (Figure S24B). We then assessed the consequences of tachypacing-dependent  $I_{\text{SK}}$ -upregulation for atrial APD by comparing the apamin effect during current-clamp experiments at baseline with those following 10-minutes of 5-Hz activation in RA Ctl-cardiomyocytes (Figure 7C and Figure S25). Apamin produced a significantly larger APD<sub>90</sub>-prolongation after 5-Hz activation (56% [38%-106%],  $n=7/5$ ) compared to cardiomyocytes without 5-Hz activation (10% [4.6%-16%],  $n=8/5$ ;  $P=0.034$ ; Figure 7C), establishing the functional relevance of tachypacing-induced  $I_{\text{SK}}$ -upregulation.

Pre-incubation with BAPTA-AM or okadaic acid abolished  $I_{\text{SK}}$  at +80 mV after 5-Hz activation and the L-type  $\text{Ca}^{2+}$ -channel inhibitor nifedipine significantly attenuated  $I_{\text{SK}}$  after 10-minutes of 5-Hz activation (Figure 7D), highlighting the importance of trans-sarcolemmal  $\text{Ca}^{2+}$  influx for  $I_{\text{SK}}$  regulation. Conversely, inhibition of calmodulin Thr80-phosphorylation with the CKII-inhibitor TBBz did not produce a larger  $I_{\text{SK}}$  compared to 5-Hz activation alone, suggesting maximal calmodulin Thr80-dephosphorylation (activation) of the sarcolemmal SK-channels after 5-Hz activation (Figure 7D). Pre-incubation with either latrunculin-A or primaquine also prevented the  $I_{\text{SK}}$ -upregulation in response to 5-Hz activation (Figure 7D, orange symbols), confirming the role of channel trafficking as an upstream regulator of SK-channel function and highlighting its key role in tachycardia-mediated  $I_{\text{SK}}$ -upregulation. Similar results were obtained at +30 mV (Figure S26).

Functional experiments cannot readily distinguish between tachypacing-induced promotion of SK-channel membrane targeting and altered channel gating. To confirm the effects of

5-Hz stimulation on channel trafficking in the absence of changes in intracellular  $\text{Ca}^{2+}$  buffering and to identify the SK-channel subunit involved, we performed immunostaining of SK-channel subunits in RA Ctl-cardiomyocytes subjected to 10 minutes of field stimulation at 0.2 or 5-Hz (Figure 8). Immunostaining revealed that tachypacing increased the membrane/cytosol ratio of SK2 (Figure 8A), but not SK1 (Figure S27) or SK3 (Figure 8B) and strongly enhanced the co-localization of SK2 with  $\alpha$ -actinin2 at the plasmalemma (Figure 8C), pointing to enhanced SK2 trafficking and  $\alpha$ -actinin2-mediated membrane targeting as key determinants of the tachypacing-mediated  $I_{\text{SK}}$ -upregulation.

## Discussion

SK-channel inhibitors have shown promising antiarrhythmic effects in various animal models, but the function and regulation of SK-channels in AF-patients is incompletely understood. Here, we demonstrate that  $I_{\text{SK}}$  is upregulated in AF and is a significant contributor to the reentry-promoting APD-abbreviation that is characteristic of the arrhythmia.  $I_{\text{SK}}$  upregulation is associated with decreased Thr80-phosphorylation of calmodulin, which increases the  $\text{Ca}^{2+}$ -affinity, and thereby the functional gating, of SK-channels; calmodulin dephosphorylation appears to be due to PP2A upregulation. Furthermore, plasma membrane levels of SK2 are higher in cAF because of altered trafficking and membrane targeting, further contributing to  $I_{\text{SK}}$  increases. Both mechanisms are engaged by short-term tachypacing in Ctl-cardiomyocytes, indicating dynamic regulation and a potential role in short-term AF self-promotion. Our results provide novel mechanistic insights relevant to the use and development of SK-channel inhibiting strategies for rhythm-control in humans.

### Molecular mechanisms underlying SK-channel remodeling

Previous work identified  $\text{Ca}^{2+}$ -dependent upregulation of SK-channel gating and trafficking in expression systems and animal models, but SK-channel regulation in the human atrium and its remodeling in AF are poorly understood. SK-channel gating is  $\text{Ca}^{2+}$ -dependent, with SK-channels located in close proximity to L-type  $\text{Ca}^{2+}$  channels and cardiac ryanodine receptor channels.<sup>46</sup> Since cardiomyocyte  $\text{Ca}^{2+}$ -handling is substantially remodeled in AF-patients,<sup>39,47</sup> we employed experimental conditions with fixed intracellular  $\text{Ca}^{2+}$  to characterize  $I_{\text{SK}}$  in the absence of confounding  $\text{Ca}^{2+}$ -handling differences. Subsequently, *in silico* modeling revealed a major contribution of  $I_{\text{SK}}$  to atrial repolarization in cAF when cAF-related  $\text{Ca}^{2+}$ -handling remodeling is simulated (Figure 2). *In vivo*, the contribution of  $I_{\text{SK}}$  may be further augmented by conditions increasing intracellular  $\text{Ca}^{2+}$ , including atrial tachycardia and sympathetic stimulation.

The  $\text{Ca}^{2+}$ -affinity of SK-channels is controlled by channel-associated calmodulin, with Thr80-phosphorylation of calmodulin decreasing  $\text{Ca}^{2+}$ -affinity and subsequently  $I_{\text{SK}}$ . We have previously identified increased PP2Ac expression in RA whole-tissue homogenates from cAF-patients.<sup>31</sup> Here, we show that PP2Ac expression is also increased in LA whole-tissue homogenates, RA-cardiomyocytes, and SK2-immunoprecipitates in RA-tissue from cAF-patients and is associated with reduced Thr80-phosphorylation of calmodulin. Moreover, the PP2A-inhibitor okadaic acid reduced  $I_{\text{SK}}$  in cAF-cardiomyocytes to the

levels observed in Ctl-cardiomyocytes (Figure 5), suggesting a key role for PP2A-mediated Thr80-dephosphorylation of SK-channel-associated calmodulin in the increased SK-channel function in cAF-patients. Previous work has identified increased single SK-channel activity in dogs with atrial tachycardia-related remodeling<sup>7</sup>; our data suggest that this might be due to PP2A-mediated Thr80-dephosphorylation of calmodulin. Future work should test this hypothesis.

The number of SK-channels targeted to the plasma membrane is an important determinant of the amplitude of  $I_{SK}$ . SK-channel trafficking and targeting are highly dynamic and depend on interactions with key cytoskeletal proteins.<sup>23,43</sup> SK2-channels recycle quickly between the plasma membrane and early (recycling) endosomes via  $Ca^{2+}$ -dependent mechanisms involving  $\alpha$ -actinin-2, which directly interacts with the C-terminus of the SK2-channel subunit, and filamin-A, an F-actin-binding phosphoprotein that cross-links actin filaments.<sup>23,43</sup> Although intracellular  $Ca^{2+}$ ,  $\alpha$ -actinin-2, filamin-A, and myosin light chain type-2 appear to play a role in SK2-channel trafficking and targeting in heterologous expression systems and animal models, their role in regulating human atrial SK-channels is poorly understood, particularly under disease conditions. Our data show increased SK-channel membrane abundance in cAF-cardiomyocytes (Figures 3 and 4), which was sensitive to inhibition of anterograde and retrograde trafficking, as was the corresponding current. Since total protein expression of SK-channels was unaltered, these data suggest an important role for SK-channel trafficking and membrane targeting in the upregulation of  $I_{SK}$  in cAF-patients. Animal studies have shown that SK-channel trafficking is promoted in response to short-term burst pacing.<sup>8</sup> Here, we reveal that 10-minutes of rapid electrical stimulation is sufficient to increase  $I_{SK}$  (Figure 7) by enhancing the number of plasmalemmal SK2 channels (Figure 8), indicating that SK2-channel trafficking is highly dynamic in human atrial cardiomyocytes and can contribute to the rapid AF-promoting repolarization abbreviation seen in patients.<sup>48</sup> This rapid turnover of SK-channels in the plasma membrane is in agreement with recent results demonstrating rapid trafficking dynamics of other ion channels.<sup>49</sup> The lack of tachycardia-dependent  $I_{SK}$  upregulation in the presence of latrunculin-A or primaquine suggests that tachycardia-dependent augmentation of channel function of the remaining SK channels is unable to overcome the reduction in channel targeting to the membrane due to trafficking inhibition.

### Controversies regarding the role of SK channels in AF

The role of  $I_{SK}$  in atrial electrophysiology and AF has been studied in a variety of models with sometimes contradictory outcomes. For instance, inhibition of  $I_{SK}$  with NS8593 reduces the duration of burst pacing-induced AF in perfused rat, guinea pig, rabbit and horse atria.<sup>11,50,51</sup> Similarly, overexpression of SK3 and knockout of the melanin synthesis enzyme dopachrome tautomerase (which increases expression of SK channels) in mice promote inducible AF, likely because of APD shortening.<sup>52,53</sup> Short-term atrial burst-pacing in rabbits enhances SK2-levels at the plasma membrane, upregulating  $I_{SK}$  and causing proarrhythmic APD shortening in rabbit pulmonary veins.<sup>8</sup> Moreover, administration of NS8593 to rats with hypertension-induced atrial remodeling<sup>50</sup> and dogs with atrial tachycardia-induced atrial remodeling<sup>7</sup> decreases the duration of induced AF, validating the proarrhythmic role of enhanced  $I_{SK}$  for the remodeled atrium. Despite

these results supporting the proarrhythmic potential of increased  $I_{SK}$ , SK2-knockout mice have prolonged atrial APs and are vulnerable to afterdepolarizations and AF induction,<sup>54</sup> and  $I_{SK}$  blockade (with apamin or UCL 1684) causes delayed repolarization, facilitates alternans and wave-breaks, promoting reentrant arrhythmia in isolated canine left atrium.<sup>55</sup> These results are consistent with the known complex relationship between repolarization and arrhythmogenesis, with either excessively rapid or excessively delayed repolarization promoting arrhythmogenesis under specific conditions.

Recent studies regarding the role of  $I_{SK}$  in AF patients have also provided differing results about the direction of change (Tables S1–S2). Both upregulation<sup>24,25</sup> and downregulation<sup>17–20</sup> of  $I_{SK}$  have been reported. Yu et al. found that apamin-sensitive  $I_{SK}$ , as well as protein and mRNA levels of SK1 and SK2, were significantly smaller in LA- and RA-cardiomyocytes from cAF- vs. Ctl-patients.<sup>26</sup> The mRNA levels of SK2 and SK3 were also lower in cAF- than in Ctl-patients and  $I_{SK}$  inhibition (with NS8593 and ICAGEN) prolonged APD in atrial cardiomyocytes from Ctl but not from cAF-patients,<sup>17</sup> suggesting a limited contribution of  $I_{SK}$  to AP-shortening in cAF. We identified non-significantly lower values of SK1 and SK2 mRNA levels in cAF vs. Ctl RA whole-tissue homogenates and significantly reduced SK2 mRNA levels in RA-cardiomyocytes, which avoid potential confounding effects from SK-subunit expression in other cell types. Thus, our data are generally consistent with previous studies at the mRNA level. In contrast, our data demonstrate an upregulation of  $I_{SK}$  in cAF vs. Ctl patients, in line with the majority of functional studies (Table S2)<sup>20,24,25,56</sup>. Our sensitivity analyses based on a population of *in silico* models also suggest that  $I_{SK}$  is an important determinant of human atrial APD<sub>90</sub>, to a level potentially greater than the slow, rapid or ultra-rapid delayed-rectifier  $K^+$  currents (Figure 3).

In general, the varying results between studies suggest heterogeneous SK-channel remodeling in AF-patients. The basis for this discrepancy is unclear, but is likely related to such factors as genetic variability, discrepancies in clinical characteristics and concomitant medication (Tables S3–S12), and differences between different types of SK-channel blockers (pore blockers like apamin versus  $Ca^{2+}$ -dependent gating modulators like NS8593). For instance, in the study by Yu et al.<sup>26</sup> there was no significant difference in LA diameter between Ctl and cAF patients. By contrast, in our study (Table S3) and others reporting larger  $I_{SK}$  in RA of cAF versus Ctl,<sup>20,56</sup> LA diameter was significantly larger in cAF versus Ctl patients. Our two-way ANOVA analyses also suggest that LA diameter might influence protein levels of different SK-channel subunits, but rather point toward lower SK-channel protein levels with larger LA diameter (Table S13; Figures S28–S30). The patients studied by Yu et al.<sup>26</sup> were also about 20 year younger than our population, pointing to potential contribution of age-dependent processes. However, other previous studies with similarly aged patient populations showed a comparably increased  $I_{SK}$  in cAF.<sup>20,56</sup> In agreement, we did not find a significant age-dependent modulation of SK-channel mRNA or protein levels, or  $I_{SK}$  in our two-way ANOVA analyses (Table S13). To define  $I_{SK}$  Skibsbjerg et al.<sup>17</sup> applied the non-selective SK-channel blockers NS9385 and ICAGEN instead of apamin. In their patch-clamp recordings they also used a ramp-pulse instead of a voltage-step protocol and a non-physiologically high extracellular  $K^+$  solution (20 mmol/L). Finally, 15 out of 22 cAF patients (68%) had a diagnosis of pulmonary hypertension, which is known to cause

right-sided HF. Our new Western blot analyses of samples from HFrEF patients suggest that ventricular dysfunction may be one contributing factor to discrepancies in the literature. Although there were no significant differences in protein levels of SK1, SK2, or SK3 between patients with and without HFrEF, nor between HFrEF patients with and without cAF (Figure S31), molecular indices of enhanced SK-channel gating (e.g. calmodulin-Thr80 dephosphorylation) were not different between cAF and Ctl patients in the presence of HFrEF (Figure S32). Similarly, our two-way ANOVA analyses suggest that presence of mitral valve insufficiency or diuretics is associated with altered protein levels of SK-channel subunits (Table S13). These differences may contribute to the divergent findings reported in the literature about SK-channel regulation.

Overall, based on the detailed between-study comparison provided in Tables S1 and S2, we believe that our current study is in agreement with the majority of available studies and, importantly, provides a mechanistic explanation for some of the discrepant results in the literature, like the apparently paradoxical increase in  $I_{SK}$  despite reduced or unchanged SK-channel subunit mRNA levels reported in the literature. Further detailed work in well-characterized patient populations is needed to confirm our current findings, with careful follow-up studies in related animal models to confirm key mechanistic inferences.

### Potential limitations

Atrial tissue was only available from patients undergoing open-heart surgery, which may not be entirely representative of the general population of AF-patients. Patients were assigned to the Ctl and cAF groups based on their clinical diagnosis. Although Ctl patients were in sinus rhythm immediately before surgery and no prior history of AF was recorded, we cannot exclude that these patients may have had undetected asymptomatic AF at some time prior to surgery. Differences in SK1-expression between Ctl- and AF/HF-patients are distinct for RA and LA,<sup>57</sup> and SK-channel expression is more pronounced around the pulmonary veins in dogs,<sup>7</sup> suggesting regional differences in SK-channel expression and remodeling. We only measured  $I_{SK}$  in RA-cardiomyocytes, but our Western blot and immunostaining data suggest similar SK-channel remodeling in RA- and LA-appendages. The more pronounced role of SK-channels near the pulmonary veins in dogs suggests that the role of SK-channels in atrial repolarization identified in the present study for RA-cardiomyocytes may be an underestimate.

There are several differences in clinical characteristics between Ctl- and cAF-patients included in the present study, which might influence SK-channel subunit protein levels (Table S13), but our experiments were not designed to quantify the impact of each clinical parameter on SK-channel function. Thus, we cannot exclude the possibility that these or other clinical factors contribute to  $I_{SK}$ -upregulation in AF-patients. However, the fact that SK-channel upregulation observed in RA cAF-cardiomyocytes can be reproduced by short-term tachypacing in RA Ctl-cardiomyocytes suggests that the molecular mechanisms of increased  $I_{SK}$  in cAF-patients are available and operative in Ctl-patients. Nevertheless, longer episodes of rapid atrial activity than the 10 minutes studied here may produce additional components of remodeling, which might contribute to, or attenuate,  $I_{SK}$  upregulation. Although 10 minutes of tachypacing were sufficient to increase  $I_{SK}$  to levels



seen in cAF-cardiomyocytes, atrial remodeling in cAF-patients is created by the combined effects of risk factors, co-morbidities and the high atrial rate itself. Since prolonged atrial tachycardia may downregulate some components of atrial remodeling,<sup>45,58</sup> it is possible that longer-term tachypacing could attenuate the contribution of SK-channel trafficking to the increased  $I_{SK}$  in cAF-patients, while activating additional control mechanisms, which, together with Thr80-dephosphorylation of calmodulin, maintain an upregulated  $I_{SK}$  in cAF-patients. Clearly extensive future work is required to explore and define additional control mechanisms of  $I_{SK}$  function, particularly in AF-paradigms. While our study is restricted to cAF-patients, these mechanisms may also apply to paroxysmal AF-patients, although this should be tested in future studies. Patients with paroxysmal AF could be instrumental for the assessment of novel control mechanisms of  $I_{SK}$  function.

It was not possible to study the functional consequences of reduced calmodulin-Thr80 phosphorylation directly in human atrial cardiomyocytes, since no single-channel current could be recorded after the formation of inside-out patches. Similarly, reversibility of the effects of latrunculin-A and primaquine could not be studied due to the required incubation times of several hours, in combination with the limited viability of isolated human atrial cardiomyocytes. Finally, our work provides insight into the mechanisms regulating established determinants of atrial arrhythmogenesis (i.e.,  $I_{SK}$ -mediated shortening of repolarization) in human atrial cardiomyocytes, suggesting a roughly comparable role to upregulated  $I_{K1}$ . However, the relative contribution of individual ion channels may be different under conditions more closely resembling AF *in vivo* and their true proarrhythmic potential or the antiarrhythmic efficacy of their inhibition requires appropriately designed controlled clinical trials in humans.

### Potential significance of our observations

Several SK-channel inhibitors have demonstrated pronounced antiarrhythmic potential in large animal models, both for acute cardioversion and for prevention of AF re-induction, suggesting a potential for SK-channel inhibition in rhythm control of AF-patients.<sup>7,9-13</sup> Ventricular effective refractory period is largely unchanged by SK-channel inhibition in most large animal models, therefore atrial selectivity is likely a beneficial characteristic of  $I_{SK}$  blockers.<sup>11-13,16</sup>

AF is associated with pronounced electrical, structural and  $Ca^{2+}$ -handling remodeling (reviewed in<sup>59-61</sup>). Patients with cAF have shorter effective refractory periods (ERPs) due to upregulation of repolarizing potassium currents and downregulation of depolarizing L-type  $Ca^{2+}$  channels, thereby promoting AF-maintaining reentrant activity. Our study is the first of which we are aware to examine in detail the molecular control mechanisms governing  $I_{SK}$  under AF conditions in human hearts. Our findings establish the role of a number of these mechanisms, including calmodulin Thr80-phosphorylation, PP2A activity and membrane trafficking and targeting. Our data indicate that SK-channel remodeling is an important contributor to ERP shortening in cAF patients, comparable to upregulation of  $I_{K1}$ , potentially contributing to AF stability. By contrast, patients with a history of paroxysmal AF from whom RA-cardiomyocytes were obtained during normal sinus rhythm, do not show ERP shortening.<sup>47,60</sup> However, our results indicate that AF, and even relatively short-term

atrial tachycardia, upregulate the current through several pathways, suggesting that  $I_{SK}$  upregulation is an important part of the AF-promoting response of atrial cardiomyocytes to sustained rapid activation, providing a plausible mechanistic basis for SK-channels as antiarrhythmic targets.<sup>62</sup>

## Conclusions

We have performed a detailed systematic analysis of the regulation of SK-channels in cAF-patients. Our findings identify rapid post-translational modification of SK-channel function, trafficking and targeting in the presence of atrial tachycardia, which shorten atrial repolarization duration and position SK-channels as potentially important contributors to self-promotion of AF in humans. These data provide novel insights into the molecular control of atrial  $I_{SK}$  in humans and a potential mechanistic framework for the development of SK-channel inhibitors for rhythm control of AF.

## Supplementary Material

Refer to Web version on PubMed Central for supplementary material.

## Acknowledgements

The authors thank Dennis Hoffmann, Annette Kötting-Dorsch, Barbara Langer, Claudia Liebetrau, Ramona Löcker, Bettina Mause, Sylvia Metze, and Simone Olesch, as well as the Imaging Center Campus Essen (ICCE) - University Duisburg Essen and the Core Facility for Integrated Microscopy (CFIM) Denmark for expert technical assistance.

## Sources of Funding

The authors' work was supported by the German Research Foundation (DFG, Do 769/4-1 to DD and ES 569/2-1 to CEM), the Netherlands Organization for Scientific Research (NWO/ZonMW Vidi 09150171910029 to JH), the Burroughs Wellcome Fund (Doris Duke Charitable Foundation "COVID-19 Fund to Retain Clinical Scientists" to SM), the Novo Nordisk foundation (Tandem Programme; #31634 to TJ), the Independent Research Fund Denmark (102900011B to AS), the Canadian Institutes of Health Research (1484011 to SN), the Heart and Stroke Foundation of Canada (22-0031958 to SN), the National Institutes of Health (R01-HL131517 to EG and DD; R01-HL136389, R01-HL089598, R01-HL163277, and R01-HL160992 to DD; 1OT2OD026580-01, R01HL141214 and P01HL141084 to EG; R00HL138160 to SM), and the European Union (large-scale integrative project MAESTRIA, No. 965286 to DD).

## Non-standard Abbreviations and Acronyms

<b>AAD</b>	Antiarrhythmic drug
<b>AF</b>	Atrial fibrillation
<b>AP</b>	Action potential
<b>APD</b>	Action potential duration
<b>cAF</b>	Long-standing persistent (chronic) atrial fibrillation
<b>CKII</b>	Casein kinase type-II
<b>Ctl</b>	Sinus rhythm control
<b>ERP</b>	Effective refractory period

<b>HF</b>	Heart failure
<b>I<sub>SK</sub></b>	Small-conductance Ca <sup>2+</sup> -activated K <sup>+</sup> current
<b>LA</b>	Left atrial
<b>PP2A</b>	Protein phosphatase type-2a
<b>RA</b>	Right atrial
<b>SK channel</b>	Small-conductance Ca <sup>2+</sup> -activated K <sup>+</sup> channel

## References

- Hindricks G, Potpara T, Dagres N, Arbelo E, Bax JJ, Blomstrom-Lundqvist C, Boriani G, Castella M, Dan GA, Dilaveris PE, et al. 2020 ESC Guidelines for the diagnosis and management of atrial fibrillation developed in collaboration with the European Association for Cardio-Thoracic Surgery (EACTS): The Task Force for the diagnosis and management of atrial fibrillation of the European Society of Cardiology (ESC) Developed with the special contribution of the European Heart Rhythm Association (EHRA) of the ESC. *Eur Heart J*. 2021;42:373–498. doi: 10.1093/eurheartj/ehaa612 [PubMed: 32860505]
- Marrouche NF, Brachmann J, Andresen D, Siebels J, Boersma L, Jordaens L, Merkely B, Pokushalov E, Sanders P, Proff J, et al. Catheter Ablation for Atrial Fibrillation with Heart Failure. *N Engl J Med*. 2018;378:417–427. doi: 10.1056/NEJMoa1707855 [PubMed: 29385358]
- Kirchhof P, Camm AJ, Goette A, Brandes A, Eckardt L, Elvan A, Fetsch T, van Gelder IC, Haase D, Haegeli LM, et al. Early Rhythm-Control Therapy in Patients with Atrial Fibrillation. *N Engl J Med*. 2020;383:1305–1316. doi: 10.1056/NEJMoa2019422 [PubMed: 32865375]
- Nattel S, Sager PT, Huser J, Heijman J, Dobrev D. Why translation from basic discoveries to clinical applications is so difficult for atrial fibrillation and possible approaches to improving it. *Cardiovasc Res*. 2021;117:1616–1631. doi: 10.1093/cvr/cvab093 [PubMed: 33769493]
- Peyronnet R, Ravens U. Atria-selective antiarrhythmic drugs in need of alliance partners. *Pharmacol Res*. 2019;145:104262. doi: 10.1016/j.phrs.2019.104262 [PubMed: 31059791]
- Heijman J, Dobrev D. Inhibition of Small-Conductance Ca<sup>2+</sup>-Activated K<sup>+</sup> Channels: The Long-Awaited Breakthrough for Antiarrhythmic Drug Therapy of Atrial Fibrillation? *Circ Arrhythm Electrophysiol*. 2017;10. doi: 10.1161/CIRCEP.117.005776
- Qi XY, Diness JG, Brundel BJ, Zhou XB, Naud P, Wu CT, Huang H, Harada M, Aflaki M, Dobrev D, et al. Role of small-conductance calcium-activated potassium channels in atrial electrophysiology and fibrillation in the dog. *Circulation*. 2014;129:430–440. doi: 10.1161/CIRCULATIONAHA.113.003019 [PubMed: 24190961]
- Ozgen N, Dun W, Sosunov EA, Anyukhovskiy EP, Hirose M, Duffy HS, Boyden PA, Rosen MR. Early electrical remodeling in rabbit pulmonary vein results from trafficking of intracellular SK2 channels to membrane sites. *Cardiovasc Res*. 2007;75:758–769. doi: 10.1016/j.cardiores.2007.05.008 [PubMed: 17588552]
- Skibsbjerg L, Bengaard AK, Uldum-Nielsen AM, Boddum K, Christ T, Jespersen T. Inhibition of Small Conductance Calcium-Activated Potassium (SK) Channels Prevents Arrhythmias in Rat Atria During beta-Adrenergic and Muscarinic Receptor Activation. *Front Physiol*. 2018;9:510. doi: 10.3389/fphys.2018.00510 [PubMed: 29922167]
- Gatta G, Sobota V, Citerni C, Diness JG, Sorensen US, Jespersen T, Bentzen BH, Zeemering S, Kuiper M, Verheule S, et al. Effective termination of atrial fibrillation by SK channel inhibition is associated with a sudden organization of fibrillatory conduction. *Europace*. 2021;23:1847–1859. doi: 10.1093/europace/euab125 [PubMed: 34080619]
- Haugaard MM, Hesselkilde EZ, Pehrson S, Carstensen H, Flethoj M, Praestegaard KF, Sorensen US, Diness JG, Grunnet M, Buhl R, et al. Pharmacologic inhibition of small-conductance calcium-activated potassium (SK) channels by NS8593 reveals atrial antiarrhythmic potential in horses. *Heart Rhythm*. 2015;12:825–835. doi: 10.1016/j.hrthm.2014.12.028 [PubMed: 25542425]

12. Diness JG, Skibsbye L, Simo-Vicens R, Santos JL, Lundegaard P, Citerni C, Sauter DRP, Bomholtz SH, Svendsen JH, Olesen SP, et al. Termination of Vernakalant-Resistant Atrial Fibrillation by Inhibition of Small-Conductance Ca<sup>2+</sup>-Activated K<sup>+</sup> Channels in Pigs. *Circ Arrhythm Electrophysiol.* 2017;10. doi: 10.1161/CIRCEP.117.005125
13. Diness JG, Kirchhoff JE, Speerschneider T, Abildgaard L, Edvardsson N, Sorensen US, Grunnet M, Bentzen BH. The K<sub>Ca2</sub> Channel Inhibitor AP30663 Selectively Increases Atrial Refractoriness, Converts Vernakalant-Resistant Atrial Fibrillation and Prevents Its Reinduction in Conscious Pigs. *Front Pharmacol.* 2020;11:159. doi: 10.3389/fphar.2020.00159 [PubMed: 32180722]
14. Roselli C, Chaffin MD, Weng LC, Aeschbacher S, Ahlberg G, Albert CM, Almgren P, Alonso A, Anderson CD, Aragam KG, et al. Multi-ethnic genome-wide association study for atrial fibrillation. *Nat Genet.* 2018;50:1225–1233. doi: 10.1038/s41588-018-0133-9 [PubMed: 29892015]
15. Gal P, Klaassen ES, Bergmann KR, Saghari M, Burggraaf J, Kemme MJB, Sylvest C, Sorensen U, Bentzen BH, Grunnet M, et al. First Clinical Study with AP30663 - a K<sub>Ca2</sub> Channel Inhibitor in Development for Conversion of Atrial Fibrillation. *Clin Transl Sci.* 2020;13:1336–1344. doi: 10.1111/cts.12835 [PubMed: 32725783]
16. Bentzen BH, Bomholtz SH, Simo-Vicens R, Folkersen L, Abildgaard L, Speerschneider T, Muthukumarasamy KM, Edvardsson N, Sorensen US, Grunnet M, et al. Mechanisms of Action of the K<sub>Ca2</sub>-Negative Modulator AP30663, a Novel Compound in Development for Treatment of Atrial Fibrillation in Man. *Front Pharmacol.* 2020;11:610. doi: 10.3389/fphar.2020.00610 [PubMed: 32477117]
17. Skibsbye L, Poulet C, Diness JG, Bentzen BH, Yuan L, Kappert U, Matschke K, Wettwer E, Ravens U, Grunnet M, et al. Small-conductance calcium-activated potassium (SK) channels contribute to action potential repolarization in human atria. *Cardiovasc Res.* 2014;103:156–167. doi: 10.1093/cvr/cvu121 [PubMed: 24817686]
18. Darkow E, Nguyen TT, Stolina M, Kari FA, Schmidt C, Wiedmann F, Baczeko I, Kohl P, Rajamani S, Ravens U, et al. Small Conductance Ca<sup>2+</sup>-Activated K<sup>+</sup> (SK) Channel mRNA Expression in Human Atrial and Ventricular Tissue: Comparison Between Donor, Atrial Fibrillation and Heart Failure Tissue. *Front Physiol.* 2021;12:650964. doi: 10.3389/fphys.2021.650964 [PubMed: 33868017]
19. Rahm AK, Gramlich D, Wieder T, Muller ME, Schoeffel A, El Tahry FA, Most P, Heimberger T, Sandke S, Weis T, et al. Trigger-Specific Remodeling of K<sub>Ca2</sub> Potassium Channels in Models of Atrial Fibrillation. *Pharmgenomics Pers Med.* 2021;14:579–590. doi: 10.2147/PGPM.S290291 [PubMed: 34045886]
20. Fan X, Yu Y, Lan H, Ou X, Yang L, Li T, Cao J, Zeng X, Li M. Ca<sup>2+</sup>/Calmodulin-Dependent Protein Kinase II (CaMKII) Increases Small-Conductance Ca<sup>2+</sup>-Activated K<sup>+</sup> Current in Patients with Chronic Atrial Fibrillation. *Med Sci Monit.* 2018;24:3011–3023. doi: 10.12659/MSM.909684 [PubMed: 29737974]
21. Bildl W, Strassmaier T, Thurm H, Andersen J, Eble S, Oliver D, Knipper M, Mann M, Schulte U, Adelman JP, et al. Protein kinase CK2 is coassembled with small conductance Ca<sup>2+</sup>-activated K<sup>+</sup> channels and regulates channel gating. *Neuron.* 2004;43:847–858. doi: 10.1016/j.neuron.2004.08.033 [PubMed: 15363395]
22. Lee WS, Ngo-Anh TJ, Bruening-Wright A, Maylie J, Adelman JP. Small conductance Ca<sup>2+</sup>-activated K<sup>+</sup> channels and calmodulin: cell surface expression and gating. *J Biol Chem.* 2003;278:25940–25946. doi: 10.1074/jbc.M302091200 [PubMed: 12734181]
23. Rafizadeh S, Zhang Z, Woltz RL, Kim HJ, Myers RE, Lu L, Tuteja D, Singapuri A, Bigdeli AA, Harchache SB, et al. Functional interaction with filamin A and intracellular Ca<sup>2+</sup> enhance the surface membrane expression of a small-conductance Ca<sup>2+</sup>-activated K<sup>+</sup> (SK2) channel. *Proc Natl Acad Sci U S A.* 2014;111:9989–9994. doi: 10.1073/pnas.1323541111 [PubMed: 24951510]
24. Li ML, Li T, Lei M, Tan XQ, Yang Y, Liu TP, Pei J, Zeng XR. [Increased small conductance calcium-activated potassium channel (SK2 channel) current in atrial myocytes of patients with persistent atrial fibrillation]. *Zhonghua Xin Xue Guan Bing Za Zhi.* 2011;39:147–151. [PubMed: 21426750]

25. Wang H, Li T, Zhang L, Yang Y, Zeng XR. [Effects of intracellular calcium alteration on SK currents in atrial cardiomyocytes from patients with atrial fibrillation]. *Zhongguo Ying Yong Sheng Li Xue Za Zhi*. 2014;30:296–300, 305. [PubMed: 25330661]
26. Yu T, Deng C, Wu R, Guo H, Zheng S, Yu X, Shan Z, Kuang S, Lin Q. Decreased expression of small-conductance  $\text{Ca}^{2+}$ -activated  $\text{K}^{+}$  channels SK1 and SK2 in human chronic atrial fibrillation. *Life Sci*. 2012;90:219–227. doi: 10.1016/j.lfs.2011.11.008 [PubMed: 22154908]
27. Voigt N, Pearman CM, Dobrev D, Dibb KM. Methods for isolating atrial cells from large mammals and humans. *J Mol Cell Cardiol*. 2015;86:187–198. doi: 10.1016/j.yjmcc.2015.07.006 [PubMed: 26186893]
28. Zhou X, Wulfsen I, Korth M, McClafferty H, Lukowski R, Shipston MJ, Ruth P, Dobrev D, Wieland T. Palmitoylation and membrane association of the stress axis regulated insert (STREX) controls BK channel regulation by protein kinase C. *J Biol Chem*. 2012;287:32161–32171. doi: 10.1074/jbc.M112.386359 [PubMed: 22843729]
29. Zhou XB, Feng YX, Sun Q, Lukowski R, Qiu Y, Spiger K, Li Z, Ruth P, Korth M, Skolnik EY, et al. Nucleoside diphosphate kinase B-activated intermediate conductance potassium channels are critical for neointima formation in mouse carotid arteries. *Arterioscler Thromb Vasc Biol*. 2015;35:1852–1861. doi: 10.1161/ATVBAHA.115.305881 [PubMed: 26088577]
30. Ni L, Lahiri SK, Nie J, Pan X, Abu-Taha I, Reynolds JO, Campbell HM, Wang H, Kamler M, Schmitz W, et al. Genetic inhibition of Nuclear Factor of Activated T-cell c2 (NFATc2) prevents atrial fibrillation in CREM transgenic mice. *Cardiovasc Res*. 2021. doi: 10.1093/cvr/cvab325
31. El-Armouche A, Boknik P, Eschenhagen T, Carrier L, Knaut M, Ravens U, Dobrev D. Molecular determinants of altered  $\text{Ca}^{2+}$  handling in human chronic atrial fibrillation. *Circulation*. 2006;114:670–680. doi: 10.1161/CIRCULATIONAHA.106.636845 [PubMed: 16894034]
32. Heijman J, Muna AP, Veleva T, Molina CE, Sutanto H, Tekook M, Wang Q, Abu-Taha IH, Gorka M, Kunzel S, et al. Atrial Myocyte NLRP3/CaMKII Nexus Forms a Substrate for Postoperative Atrial Fibrillation. *Circ Res*. 2020;127:1036–1055. doi: 10.1161/CIRCRESAHA.120.316710 [PubMed: 32762493]
33. Chiang DY, Lebesgue N, Beavers DL, Alsina KM, Damen JM, Voigt N, Dobrev D, Wehrens XH, Scholten A. Alterations in the interactome of serine/threonine protein phosphatase type-1 in atrial fibrillation patients. *J Am Coll Cardiol*. 2015;65:163–173. doi: 10.1016/j.jacc.2014.10.042 [PubMed: 25593058]
34. Grandi E, Pandit SV, Voigt N, Workman AJ, Dobrev D, Jalife J, Bers DM. Human atrial action potential and  $\text{Ca}^{2+}$  model: sinus rhythm and chronic atrial fibrillation. *Circ Res*. 2011;109:1055–1066. doi: 10.1161/CIRCRESAHA.111.253955 [PubMed: 21921263]
35. Voigt N, Heijman J, Trausch A, Mintert-Jancke E, Pott L, Ravens U, Dobrev D. Impaired  $\text{Na}^{+}$ -dependent regulation of acetylcholine-activated inward-rectifier  $\text{K}^{+}$  current modulates action potential rate dependence in patients with chronic atrial fibrillation. *J Mol Cell Cardiol*. 2013;61:142–152. doi: 10.1016/j.yjmcc.2013.03.011 [PubMed: 23531443]
36. Schmidt C, Wiedmann F, Voigt N, Zhou XB, Heijman J, Lang S, Albert V, Kallenberger S, Ruhparwar A, Szabo G, et al. Upregulation of  $\text{K}_{2p3.1}$   $\text{K}^{+}$  Current Causes Action Potential Shortening in Patients With Chronic Atrial Fibrillation. *Circulation*. 2015;132:82–92. doi: 10.1161/CIRCULATIONAHA.114.012657 [PubMed: 25951834]
37. Sobie EA. Parameter sensitivity analysis in electrophysiological models using multivariable regression. *Biophys J*. 2009;96:1264–1274. doi: 10.1016/j.bpj.2008.10.056 [PubMed: 19217846]
38. Sikkil MB, Francis DP, Howard J, Gordon F, Rowlands C, Peters NS, Lyon AR, Harding SE, MacLeod KT. Hierarchical statistical techniques are necessary to draw reliable conclusions from analysis of isolated cardiomyocyte studies. *Cardiovasc Res*. 2017;113:1743–1752. doi: 10.1093/cvr/cvx151 [PubMed: 29016722]
39. Voigt N, Li N, Wang Q, Wang W, Trafford AW, Abu-Taha I, Sun Q, Wieland T, Ravens U, Nattel S, et al. Enhanced sarcoplasmic reticulum  $\text{Ca}^{2+}$  leak and increased  $\text{Na}^{+}$ - $\text{Ca}^{2+}$  exchanger function underlie delayed afterdepolarizations in patients with chronic atrial fibrillation. *Circulation*. 2012;125:2059–2070. doi: 10.1161/CIRCULATIONAHA.111.067306 [PubMed: 22456474]
40. Blatz AL, Magleby KL. Single apamin-blocked  $\text{Ca}^{2+}$ -activated  $\text{K}^{+}$  channels of small conductance in cultured rat skeletal muscle. *Nature*. 1986;323:718–720. doi: 10.1038/323718a0 [PubMed: 2430185]

41. Eichhorn B, Dobrev D. Vascular large conductance calcium-activated potassium channels: functional role and therapeutic potential. *Naunyn Schmiedebergs Arch Pharmacol.* 2007;376:145–155. doi: 10.1007/s00210-007-0193-3 [PubMed: 17932654]
42. Faber ES, Delaney AJ, Power JM, Sedlak PL, Crane JW, Sah P. Modulation of SK channel trafficking by beta adrenoceptors enhances excitatory synaptic transmission and plasticity in the amygdala. *J Neurosci.* 2008;28:10803–10813. doi: 10.1523/JNEUROSCI.1796-08.2008 [PubMed: 18945888]
43. Zhang Z, Ledford HA, Park S, Wang W, Rafizadeh S, Kim HJ, Xu W, Lu L, Lau VC, Knowlton AA, et al. Distinct subcellular mechanisms for the enhancement of the surface membrane expression of SK2 channel by its interacting proteins, alpha-actinin2 and filamin A. *J Physiol.* 2017;595:2271–2284. doi: 10.1113/JP272942 [PubMed: 27779751]
44. Lu L, Timofeyev V, Li N, Rafizadeh S, Singapuri A, Harris TR, Chiamvimonvat N. Alpha-actinin2 cytoskeletal protein is required for the functional membrane localization of a Ca<sup>2+</sup>-activated K<sup>+</sup> channel (SK2 channel). *Proc Natl Acad Sci U S A.* 2009;106:18402–18407. doi: 10.1073/pnas.0908207106 [PubMed: 19815520]
45. Qi XY, Yeh YH, Xiao L, Burstein B, Maguy A, Chartier D, Villeneuve LR, Brundel BJ, Dobrev D, Nattel S. Cellular signaling underlying atrial tachycardia remodeling of L-type calcium current. *Circ Res.* 2008;103:845–854. doi: 10.1161/CIRCRESAHA.108.175463 [PubMed: 18723446]
46. Zhang XD, Coulibaly ZA, Chen WC, Ledford HA, Lee JH, Sirish P, Dai G, Jian Z, Chuang F, Brust-Mascher I, et al. Coupling of SK channels, L-type Ca<sup>2+</sup> channels, and ryanodine receptors in cardiomyocytes. *Sci Rep.* 2018;8:4670. doi: 10.1038/s41598-018-22843-3 [PubMed: 29549309]
47. Voigt N, Heijman J, Wang Q, Chiang DY, Li N, Karck M, Wehrens XHT, Nattel S, Dobrev D. Cellular and molecular mechanisms of atrial arrhythmogenesis in patients with paroxysmal atrial fibrillation. *Circulation.* 2014;129:145–156. doi: 10.1161/CIRCULATIONAHA.113.006641 [PubMed: 24249718]
48. Daoud EG, Bogun F, Goyal R, Harvey M, Man KC, Strickberger SA, Morady F. Effect of atrial fibrillation on atrial refractoriness in humans. *Circulation.* 1996;94:1600–1606. doi: 10.1161/01.cir.94.7.1600 [PubMed: 8840850]
49. Kanner SA, Jain A, Colecraft HM. Development of a High-Throughput Flow Cytometry Assay to Monitor Defective Trafficking and Rescue of Long QT2 Mutant hERG Channels. *Front Physiol.* 2018;9:397. doi: 10.3389/fphys.2018.00397 [PubMed: 29725305]
50. Diness JG, Skibsbye L, Jespersen T, Bartels ED, Sorensen US, Hansen RS, Grunnet M. Effects on atrial fibrillation in aged hypertensive rats by Ca<sup>2+</sup>-activated K<sup>+</sup> channel inhibition. *Hypertension.* 2011;57:1129–1135. doi: 10.1161/HYPERTENSIONAHA.111.170613 [PubMed: 21502564]
51. Diness JG, Sorensen US, Nissen JD, Al-Shahib B, Jespersen T, Grunnet M, Hansen RS. Inhibition of small-conductance Ca<sup>2+</sup>-activated K<sup>+</sup> channels terminates and protects against atrial fibrillation. *Circ Arrhythm Electrophysiol.* 2010;3:380–390. doi: 10.1161/CIRCEP.110.957407 [PubMed: 20562443]
52. Mahida S, Mills RW, Tucker NR, Simonson B, Macri V, Lemoine MD, Das S, Milan DJ, Ellinor PT. Overexpression of KCNN3 results in sudden cardiac death. *Cardiovasc Res.* 2014;101:326–334. doi: 10.1093/cvr/cvt269 [PubMed: 24296650]
53. Tsai WC, Chan YH, Hsueh CH, Everett TH, Chang PC, Choi EK, Olaopa MA, Lin SF, Shen C, Kudela MA, et al. Small conductance calcium-activated potassium current and the mechanism of atrial arrhythmia in mice with dysfunctional melanocyte-like cells. *Heart Rhythm.* 2016;13:1527–1535. doi: 10.1016/j.hrthm.2016.03.011 [PubMed: 26961301]
54. Li N, Timofeyev V, Tuteja D, Xu D, Lu L, Zhang Q, Zhang Z, Singapuri A, Albert TR, Rajagopal AV, et al. Ablation of a Ca<sup>2+</sup>-activated K<sup>+</sup> channel (SK2 channel) results in action potential prolongation in atrial myocytes and atrial fibrillation. *J Physiol.* 2009;587:1087–1100. doi: 10.1113/jphysiol.2008.167718 [PubMed: 19139040]
55. Hsueh CH, Chang PC, Hsieh YC, Reher T, Chen PS, Lin SF. Proarrhythmic effect of blocking the small conductance calcium activated potassium channel in isolated canine left atrium. *Heart Rhythm.* 2013;10:891–898. doi: 10.1016/j.hrthm.2013.01.033 [PubMed: 23376397]
56. Yu Y, Luo D, Li Z, Zhang J, Li F, Qiao J, Yu F, Li M. Inhibitory Effects of Dronedronone on Small Conductance Calcium Activated Potassium Channels in Patients with Chronic Atrial Fibrillation:



- Comparison to Amiodarone. *Med Sci Monit.* 2020;26:e924215. doi: 10.12659/MSM.924215 [PubMed: 32470968]
57. Rahm AK, Wieder T, Gramlich D, Muller ME, Wunsch MN, El Tahry FA, Heimberger T, Sandke S, Weis T, Most P, et al. Differential regulation of KCa2.1 (KCNN1) K<sup>+</sup> channel expression by histone deacetylases in atrial fibrillation with concomitant heart failure. *Physiol Rep.* 2021;9:e14835. doi: 10.14814/phy2.14835 [PubMed: 34111326]
  58. Greiser M, Kerfant BG, Williams GS, Voigt N, Harks E, Dibb KM, Giese A, Meszaros J, Verheule S, Ravens U, et al. Tachycardia-induced silencing of subcellular Ca<sup>2+</sup> signaling in atrial myocytes. *J Clin Invest.* 2014;124:4759–4772. doi: 10.1172/JCI70102 [PubMed: 25329692]
  59. Dobrev D, Ravens U. Remodeling of cardiomyocyte ion channels in human atrial fibrillation. *Basic Res Cardiol.* 2003;98:137–148. doi: 10.1007/s00395-003-0409-8 [PubMed: 12883831]
  60. Heijman J, Voigt N, Nattel S, Dobrev D. Cellular and molecular electrophysiology of atrial fibrillation initiation, maintenance, and progression. *Circ Res.* 2014;114:1483–1499. doi: 10.1161/CIRCRESAHA.114.302226 [PubMed: 24763466]
  61. Molina CE, Abu-Taha IH, Wang Q, Rosello-Diez E, Kamler M, Nattel S, Ravens U, Wehrens XHT, Hove-Madsen L, Heijman J, et al. Profibrotic, Electrical, and Calcium-Handling Remodeling of the Atria in Heart Failure Patients With and Without Atrial Fibrillation. *Front Physiol.* 2018;9:1383. doi: 10.3389/fphys.2018.01383 [PubMed: 30356673]
  62. Nattel S, Heijman J, Zhou L, Dobrev D. Molecular Basis of Atrial Fibrillation Pathophysiology and Therapy: A Translational Perspective. *Circ Res.* 2020;127:51–72. doi: 10.1161/CIRCRESAHA.120.316363 [PubMed: 32717172]
  63. Chua SK, Chang PC, Maruyama M, Turker I, Shinohara T, Shen MJ, Chen Z, Shen C, Rubart-von der Lohe M, Lopshire JC, et al. Small-conductance calcium-activated potassium channel and recurrent ventricular fibrillation in failing rabbit ventricles. *Circ Res.* 2011;108:971–979. doi: 10.1161/CIRCRESAHA.110.238386 [PubMed: 21350217]
  64. Ni Y, Wang T, Zhuo X, Song B, Zhang J, Wei F, Bai H, Wang X, Yang D, Gao L, et al. Bisoprolol reversed small conductance calcium-activated potassium channel (SK) remodeling in a volume-overload rat model. *Mol Cell Biochem.* 2013;384:95–103. doi: 10.1007/s11010-013-1785-5 [PubMed: 23975505]
  65. Caballero R, de la Fuente MG, Gomez R, Barana A, Amoros I, Dolz-Gaiton P, Osuna L, Almendral J, Atienza F, Fernandez-Aviles F, et al. In humans, chronic atrial fibrillation decreases the transient outward current and ultrarapid component of the delayed rectifier current differentially on each atria and increases the slow component of the delayed rectifier current in both. *J Am Coll Cardiol.* 2010;55:2346–2354. doi: 10.1016/j.jacc.2010.02.028 [PubMed: 20488306]
  66. Neef S, Dybkova N, Sossalla S, Ort KR, Fluschnik N, Neumann K, Seipelt R, Schondube FA, Hasenfuss G, Maier LS. CaMKII-dependent diastolic SR Ca<sup>2+</sup> leak and elevated diastolic Ca<sup>2+</sup> levels in right atrial myocardium of patients with atrial fibrillation. *Circ Res.* 2010;106:1134–1144. doi: 10.1161/CIRCRESAHA.109.203836 [PubMed: 20056922]
  67. Kernik DC, Morotti S, Wu H, Garg P, Duff HJ, Kurokawa J, Jalife J, Wu JC, Grandi E, Clancy CE. A computational model of induced pluripotent stem-cell derived cardiomyocytes incorporating experimental variability from multiple data sources. *J Physiol.* 2019;597:4533–4564. doi: 10.1113/JP277724 [PubMed: 31278749]
  68. Van Wagoner DR, Pond AL, Lamorgese M, Rossie SS, McCarthy PM, Nerbonne JM. Atrial L-type Ca<sup>2+</sup> currents and human atrial fibrillation. *Circ Res.* 1999;85:428–436. doi: 10.1161/01.res.85.5.428 [PubMed: 10473672]
  69. Bosch RF, Zeng X, Grammer JB, Popovic K, Mewis C, Kuhlkamp V. Ionic mechanisms of electrical remodeling in human atrial fibrillation. *Cardiovasc Res.* 1999;44:121–131. doi: 10.1016/s0008-6363(99)00178-9 [PubMed: 10615396]
  70. Workman AJ, Kane KA, Rankin AC. The contribution of ionic currents to changes in refractoriness of human atrial myocytes associated with chronic atrial fibrillation. *Cardiovasc Res.* 2001;52:226–235. doi: 10.1016/s0008-6363(01)00380-7 [PubMed: 11684070]

## Novelty and Significance

### What is known?

- Small-conductance  $\text{Ca}^{2+}$ -activated  $\text{K}^+$  (SK)-channels show a predominant atrial expression in humans, making them interesting candidates for pharmacological rhythm control of atrial fibrillation (AF).
- SK-channel inhibitors have significant antiarrhythmic effects in AF animal models, but there are conflicting data on the AF-associated changes in SK-current ( $I_{\text{SK}}$ ) in humans.
- SK-channels can undergo various forms of post-translational regulation, affecting channel gating and membrane localization, but the molecular mechanisms operative in human atrial cardiomyocytes of AF-patients are poorly defined.

### What new information does this article contribute?

- SK current ( $I_{\text{SK}}$ ) is increased in patients with long-standing persistent (chronic) AF (cAF) with no changes in SK-channel subunit expression.
- The AF-related upregulation of  $I_{\text{SK}}$  is associated with PP2A-mediated calmodulin-Thr80 dephosphorylation, promoting enhanced channel gating, and increased membrane trafficking and targeting of SK-channels in both left- and right-atria.
- Short-term (10-minutes) rapid electrical activation at 5-Hz upregulates  $I_{\text{SK}}$  by increasing plasmalemmal SK2-targeting in cardiomyocytes from Ctl-patients to levels observed in cAF-patients.

There remains a significant unmet clinical need for novel safer, more effective antiarrhythmic drugs. SK-channel inhibitors have significant antiarrhythmic effects in AF animal models, but regulation of SK-channels in AF-patients is poorly understood. Here, we identified a significant upregulation of  $I_{\text{SK}}$  in atrial cardiomyocytes from cAF-patients and detailed the underlying molecular mechanisms. We provide the first demonstration of AF-associated PP2A upregulation, calmodulin Thr80-dephosphorylation, and PP2A-mediated  $I_{\text{SK}}$  regulation in human atrial cardiomyocytes. Furthermore, we establish trafficking-dependent upregulation of SK-channel membrane targeting in AF patients as a second factor promoting increased  $I_{\text{SK}}$ . We present an improved human atrial cardiomyocyte computational model and together with experimental action-potential recordings demonstrate the importance of  $I_{\text{SK}}$  upregulation for shortening of the atrial effective refractory period. Finally, we revealed a rapid upregulation of plasmalemmal SK2-membrane targeting and  $I_{\text{SK}}$  after 10 minutes of atrial tachycardia, which is also sensitive to inhibition of PP2A and trafficking pathways. Together, our findings position SK-channels as potentially important contributors to self-promotion of AF in humans, provide novel insight into the molecular control of  $I_{\text{SK}}$  and provide a mechanistic rationale for the development of SK-channel inhibitors for rhythm control of AF.

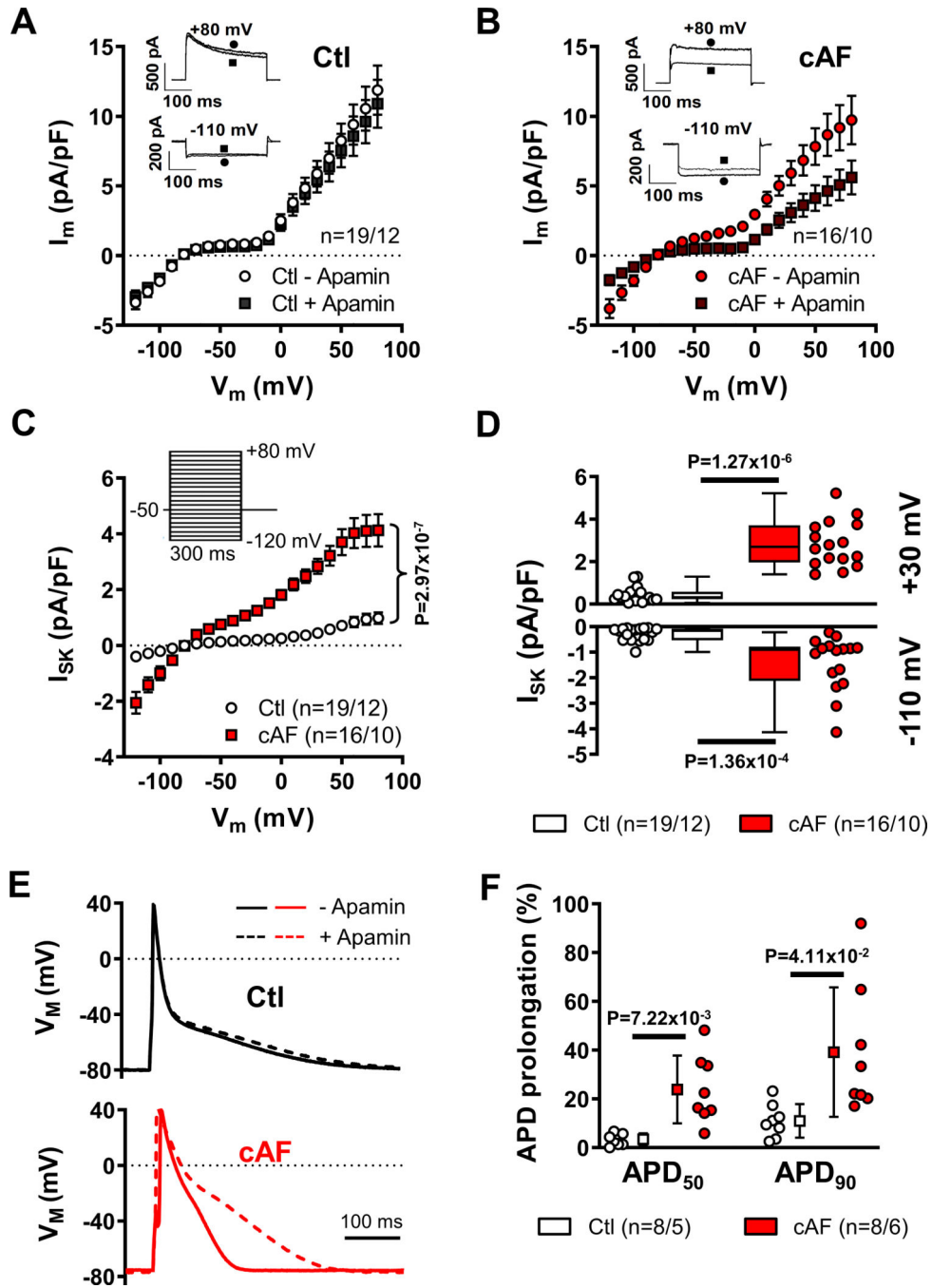


**Figure 1. Small-conductance Ca<sup>2+</sup>-activated K<sup>+</sup>-current (ISK) in right-atrial (RA) Ctl- and cAF-cardiomyocytes.**

**A-B**, Membrane current during 300-ms voltage-clamp pulses from -120 mV to +80 mV with 500-nmol/L intracellular Ca<sup>2+</sup> in the absence or presence of 100-nmol/L apamin in Ctl- or cAF-cardiomyocytes. Insets show representative examples at -110 mV and +80 mV. **C**, Voltage-dependence of apamin-sensitive  $I_{SK}$  in Ctl (white symbols) or cAF (red symbols). **D**, Comparison of apamin-sensitive  $I_{SK}$  between Ctl and cAF at +30 mV and -110 mV. N-numbers indicate numbers of cardiomyocytes/patients. **E**, Representative action

potentials in the absence or presence of 100-nmol/L apamin in a Ctl- or cAF-cardiomyocyte in the presence of 500-nmol/L intracellular  $\text{Ca}^{2+}$ . **F**, Relative apamin-induced prolongation of action potential duration at 50% or 90% of repolarization ( $\text{APD}_{50}$  and  $\text{APD}_{90}$ ) in Ctl and cAF. *P*-values are based on two-way ANOVA with repeated measures for  $V_M$  (**C**) or multilevel mixed models with log-transformed data (**D**) or regular data (**F**) to account for non-independent measurements in multiple cells from individual patients.

Author Manuscript

Author Manuscript

Author Manuscript

Author Manuscript

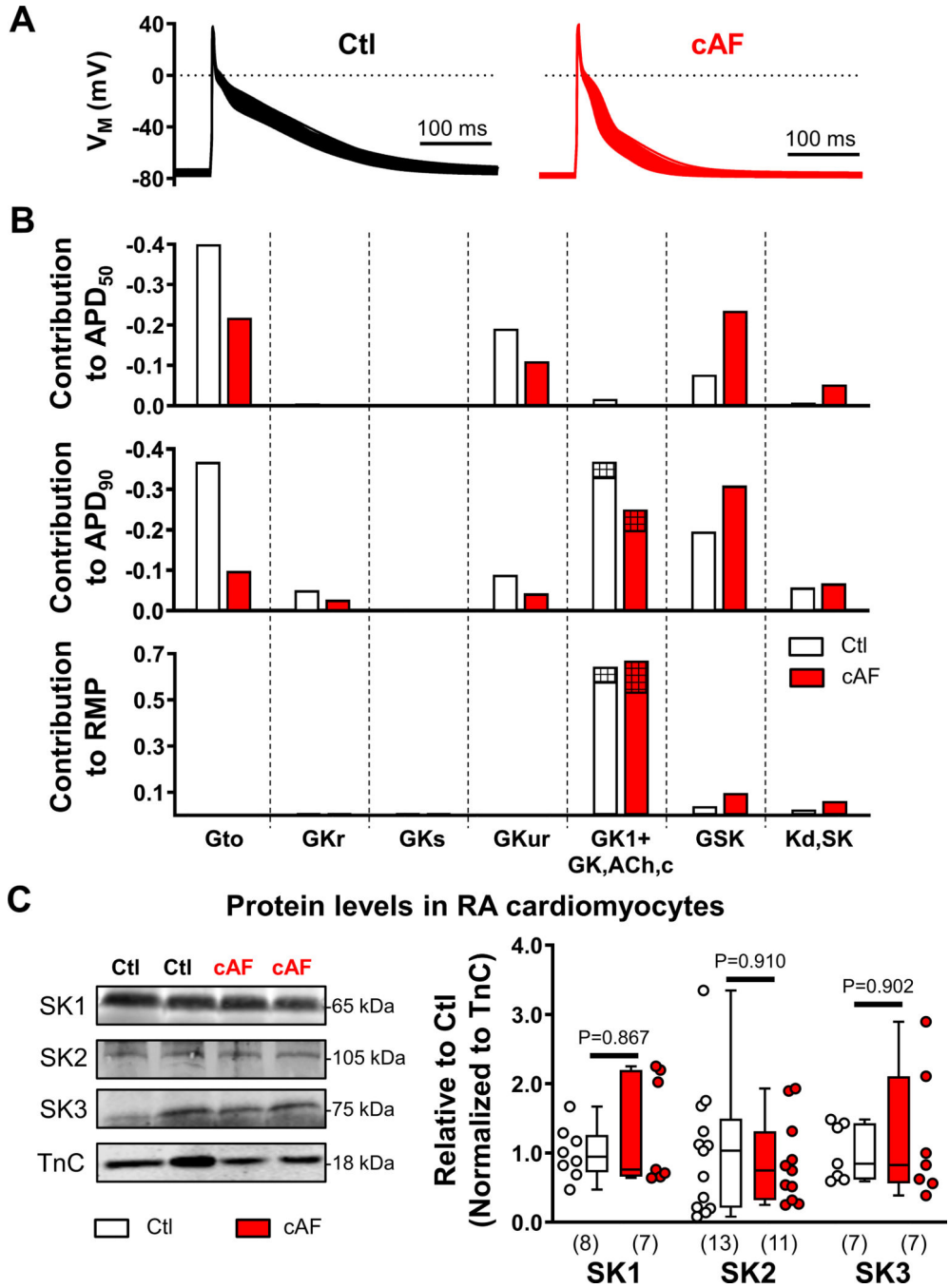


**Figure 2. Relative contribution of small-conductance Ca<sup>2+</sup>-activated K<sup>+</sup> (SK)-current and other K<sup>+</sup>-currents to action potential (AP) duration and resting membrane potential (RMP) in the in silico human atrial cardiomyocyte model and protein levels of SK channel subunits in right-atrial (RA)-cardiomyocytes from Ctl- and cAF-patients.**

**A**, Steady-state APs during 1-Hz pacing in the populations of Ctl (left) and cAF (right) models. **B**, Relative contribution of the maximal conductance of the transient-outward K<sup>+</sup>-current (Gto); rapid, slow or ultra-rapid delayed-rectifier K<sup>+</sup>-currents (GKr, GKs and GKur, respectively); basal inward-rectifier K<sup>+</sup>-current (composed of GK1, empty bars; and constitutively-active acetylcholine-activated inward-rectifier K<sup>+</sup> current GK,ACh,c, hatched

bars, 10% in Ctl and 20% in cAF); and SK-current (GSK), as well as affinity of SK-current for intracellular  $\text{Ca}^{2+}$  ( $K_d, \text{SK}$ ) to AP duration at 50%- or 90%-repolarization ( $\text{APD}_{50}$ ;  $\text{APD}_{90}$ ) or RMP in Ctl (white bars) or cAF (red bars) model populations. Each bar represents a regression coefficient linking a certain model parameter to a certain AP feature. The coefficient can be used to predict the value of each AP feature after applying a known perturbation in the baseline value of the model parameter, as detailed in the online-only Data Supplement. **C**, Representative Western blots (left) and quantification of SK1, SK2 and SK3 proteins in RA-cardiomyocytes from Ctl- and cAF-patients. N-numbers indicate number of patients. *P*-values are based on Mann-Whitney tests comparing Ctl vs. cAF.



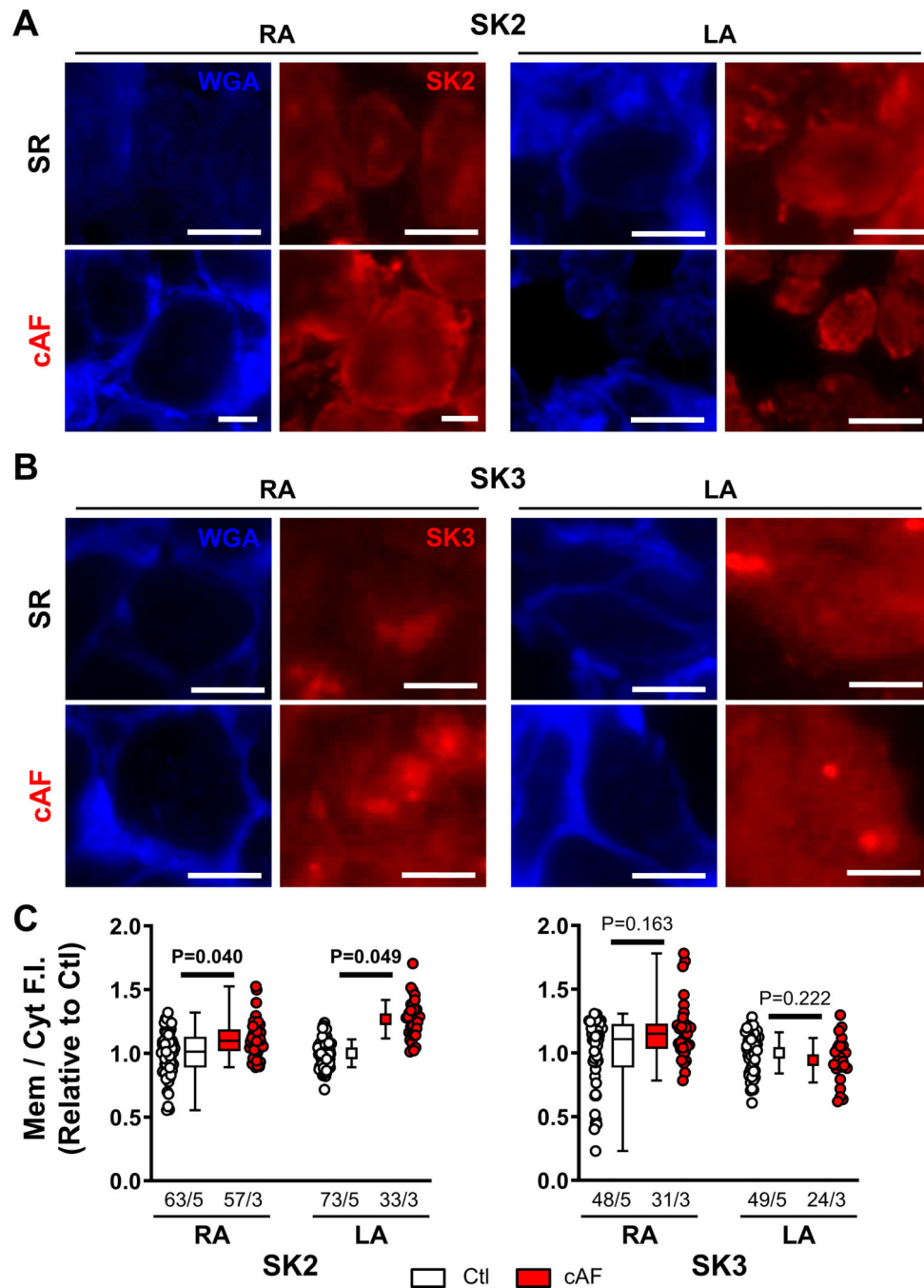


**Figure 3. Immunostaining of small-conductance Ca<sup>2+</sup>-activated K<sup>+</sup> (SK)-channel isoforms in human atrial cardiomyocytes of right- and left-atrial (RA and LA) tissue slices.**

**A**, Representative wheat germ agglutinin (WGA) and SK2 staining in RA (left) and LA (right) tissue slices of Ctl (top) and cAF patients (bottom). Scale bars indicate 10- $\mu$ m. **B**, Similar to panel A for WGA and SK3. **C**, Quantification of average fluorescence intensity (F.I.) of SK2 (left) or SK3 (right) at the membrane compared to the cytosol in the RA and LA for Ctl- and cAF-patients. Membrane regions were delineated based on WGA staining as shown in Figures S16–S18. Data are normalized to corresponding Ctl-cardiomyocytes.

N-numbers indicate numbers of cardiomyocytes/patients. *P*-values are based on multilevel mixed models with log-transformed data (RA) or regular data (LA) to account for non-independent measurements in multiple cells from individual patients.

Author Manuscript

Author Manuscript

Author Manuscript

Author Manuscript

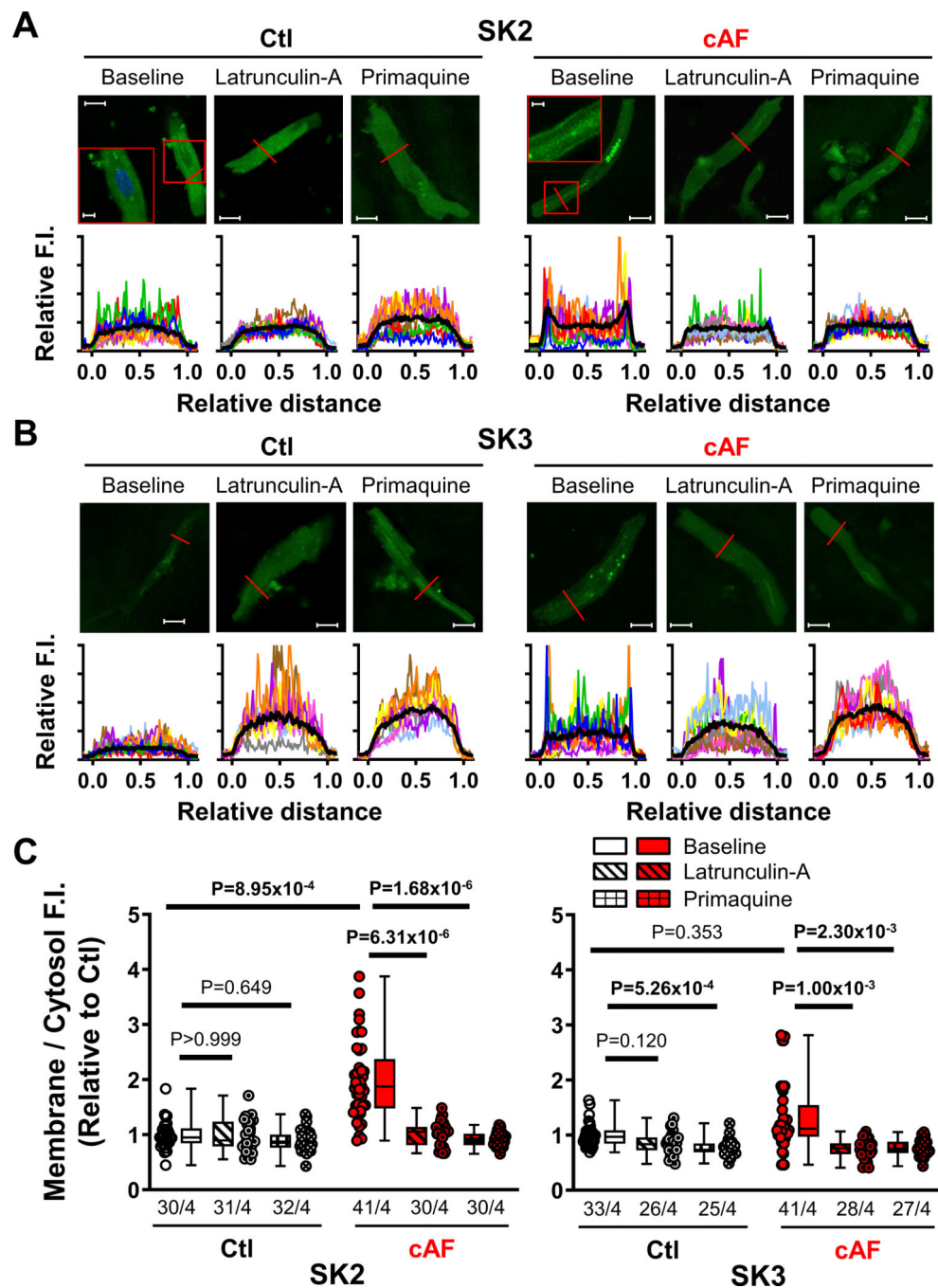


**Figure 4. Membrane localization and trafficking of small-conductance Ca<sup>2+</sup>-activated K<sup>+</sup> (SK)-channel isoforms.**

**A**, Representative immunocytochemistry of SK2 in right-atrial (RA)-cardiomyocytes from Ctrl- and cAF-patients at baseline or after inhibition of anterograde or retrograde protein trafficking with latrunculin-A (1- $\mu$ mol/L for 2-hours) or primaquine (120- $\mu$ mol/L for 4-hours), respectively. Lower panels show transversal line profiles of fluorescence intensity (F.I.) for all cardiomyocytes (thin colored lines), as well as the average across all cells (thick black lines). Scale bars indicate 15- $\mu$ m (5- $\mu$ m in the insets). **B**, Similar to panel A

for SK3. Data for SK1 are provided in Figure S19. C, Average F.I. of SK2 (left) or SK3 (right) at the membrane (first and last 10% of cell width) compared to the cytosol (middle 80%) for Ctl and cAF with or without latrunculin-A (diagonal-patterned bars) or primaquine (hashed bars). Data are normalized to Ctl-cardiomyocytes at baseline. N-numbers indicate numbers of cardiomyocytes/patients. *P*-values are based on multilevel mixed models with log-transformed data to account for non-independent measurements in multiple cells from individual patients and are Bonferroni-corrected to account for multiple comparisons.

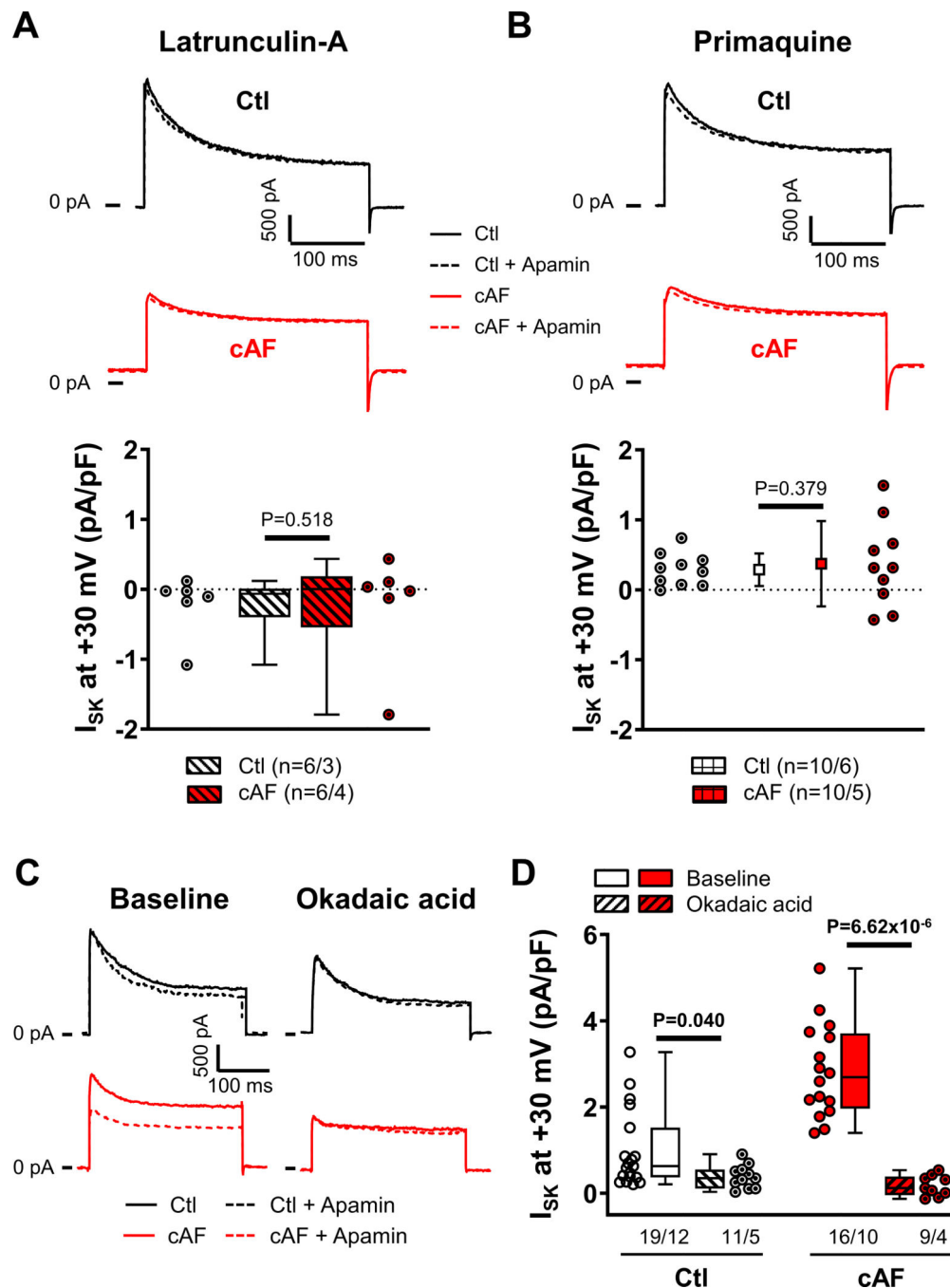


**Figure 5. Trafficking- and phosphorylation-dependent regulation of small-conductance Ca<sup>2+</sup>-activated K<sup>+</sup>-current (ISK) in right-atrial (RA)-cardiomyocytes from Ctl- and cAF-patients.** **A**, Representative examples (top) of membrane current during depolarizing pulses to +80 mV in the absence or presence of 100-nmol/L apamin and group data of apamin-sensitive I<sub>SK</sub> (bottom) at +30 mV in Ctl- and cAF-cardiomyocytes in the presence of the actin-depolymerizing agent latrunculin-A (1- $\mu$ mol/L for 2-hours), which modulates anterograde protein trafficking. **B**, Similar to panel A in the presence of the early (recycling) endosomes inhibitor primaquine (120- $\mu$ mol/L for 4-hours), which inhibits retrograde protein trafficking.

**C**, Membrane current during depolarizing pulses to +80 mV in the absence (solid lines) or presence (dashed lines) of 100-nmol/L apamin for Ctl- and cAF-cardiomyocytes at baseline (left) or in the presence of PP2A-inhibition with 10-nmol/L okadaic acid (right). **D**, Quantification of apamin-sensitive  $I_{SK}$  at +30 mV in atrial cardiomyocytes from Ctl- and cAF-patients at baseline (open bars) or in the presence of okadaic acid (diagonal-patterned bars). N-numbers indicate numbers of cardiomyocytes/patients. *P*-values are based on multilevel mixed models with log-transformed data (**A**,**D**) or regular data (**B**) to account for non-independent measurements in multiple cells from individual patients. *P*-values in (**D**) were Bonferroni-corrected to account for multiple comparisons.



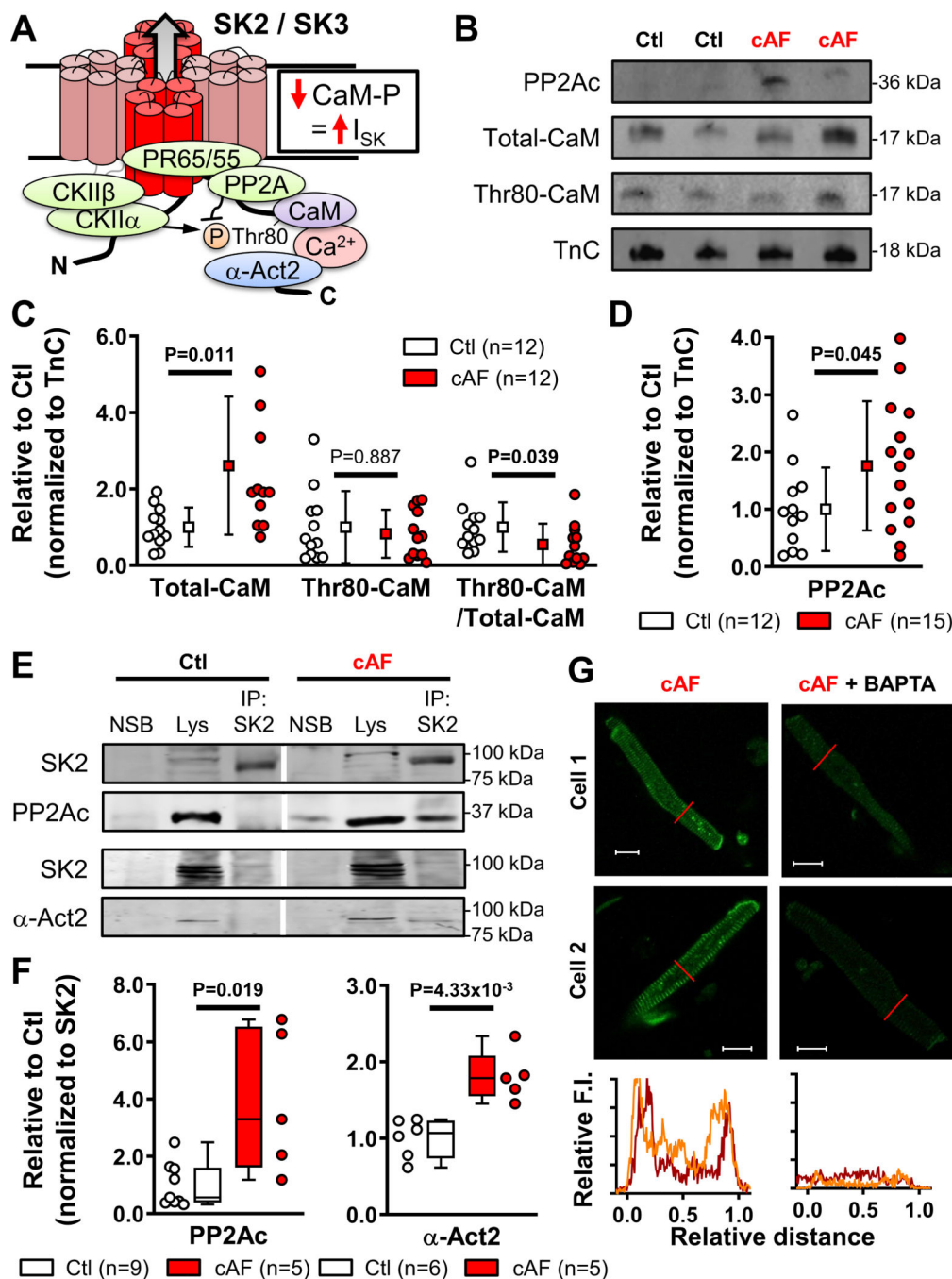


**Figure 6. Ca<sup>2+</sup>/calmodulin (CaM)-dependent regulation of small-conductance Ca<sup>2+</sup>-activated K<sup>+</sup> (SK)-channels in human right atria (RA).**

**A**, Schematic representation of the SK-channel macromolecular complex, including phosphorylation-dependent regulation of CaM. **B**, Western blots of the catalytic subunit of protein phosphatase-2a (PP2Ac), total CaM and Thr80-phosphorylated CaM in RA-cardiomyocytes from Ctl- and cAF-patients. Troponin-C (TnC) was used as loading control. **C**, Quantification of total and Thr80-phosphorylated calmodulin, as well as relative phosphorylation ratio in RA-cardiomyocytes from Ctl- and cAF-patients. **D**,

Quantification of PP2Ac protein levels in RA-cardiomyocytes from Ctl- and cAF-patients. **E**, Representative co-immunoprecipitation experiments showing Western blots of SK2 and PP2Ac or SK2 and  $\alpha$ -actinin-2 ( $\alpha$ -Act2) in lysates (lys) or SK2-immunoprecipitates from RA whole-tissue homogenates of Ctl- or cAF-patients, together with negative control for non-specific binding (NSB). Vertical white lines delineate separate regions on the same gel. **F**, Quantification of SK2-associated PP2Ac (left) or  $\alpha$ -Act2 in RA whole-tissue homogenates of Ctl- and cAF-patients. **G**, Representative immunostaining and associated line scans (bottom) of SK2 in RA-cardiomyocytes from cAF patients incubated with (right) or without BAPTA-AM (25  $\mu$ mol/L for 5-hours, left). N-numbers indicate numbers of patients. *P*-values are based on unpaired Student's *t*-test (**C,D**) or Mann-Whitney tests (**F**).

Author Manuscript

Author Manuscript

Author Manuscript

Author Manuscript

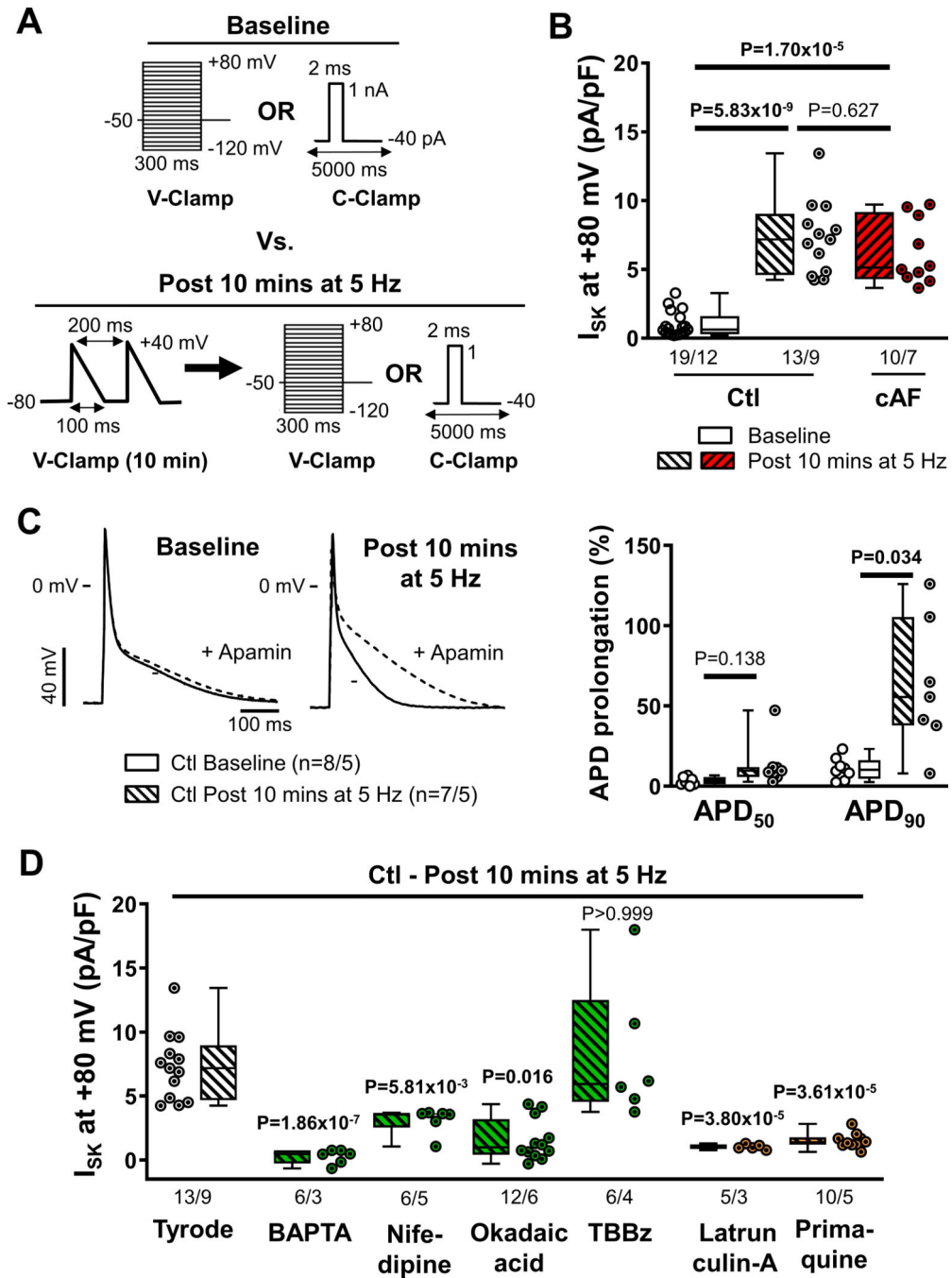


**Figure 7. Tachycardia-dependent upregulation of small-conductance Ca<sup>2+</sup>-activated K<sup>+</sup> (SK)-channels.**

**A**, Voltage- or current-clamp protocols (V-Clamp and C-clamp, respectively) comparing baseline conditions with conditions after 10-minutes of depolarizing V-Clamp pulses mimicking action potentials (APs) delivered at 5-Hz. **B**, Apamin (100-nmol/L)-sensitive  $I_{SK}$  at +80 mV in right-atrial (RA)-cardiomyocytes from Ctl-patients at baseline (open symbols) and from RA-cardiomyocytes from Ctl- or cAF-patients after 10-minutes of 5-Hz activation (diagonal-patterned bars). **C**, Representative APs in RA-cardiomyocytes from Ctl-patients at

baseline or after 10-minutes stimulation at 5-Hz in the absence or presence of apamin (left), as well as apamin-induced prolongation of APD at 50% or 90% of repolarization (APD<sub>50</sub> and APD<sub>90</sub>, respectively). **D**, Apamin-sensitive I<sub>SK</sub> at +80 mV in RA-cardiomyocytes from Ctl-patients after 10-minutes of 5-Hz activation after pre-incubation with the Ca<sup>2+</sup>-chelator BAPTA (30-μmol/L for 1-hour), L-type Ca<sup>2+</sup>-channel blocker nifedipine (1-μmol/L for 3 mins), PP2A-inhibitor okadaic acid (10-nmol/L for 1-hour) or casein kinase type-II inhibitor TBBz (10-μmol/L for 1-hour) (green bars; all affecting SK-channel gating), or latrunculin-A (1-μmol/L for 2-hours) and primaquine (120-μmol/L for 4-hours) (orange bars; both affecting SK-channel trafficking). N-numbers indicate numbers of cardiomyocytes/patients. P-values are based on multilevel mixed models with log-transformed data to account for non-independent measurements in multiple cells from individual patients and are Bonferroni-corrected to account for multiple comparisons.

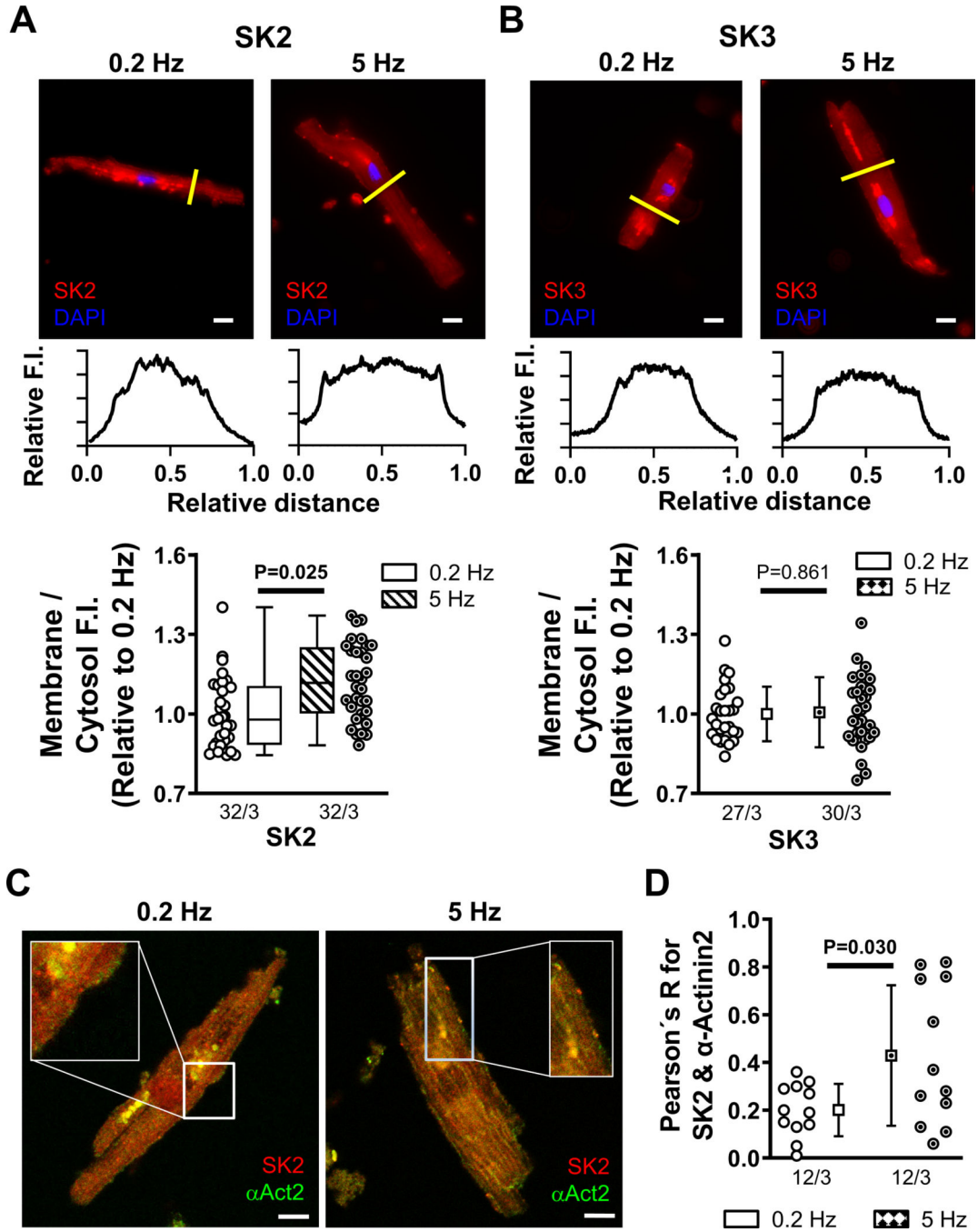


**Figure 8. Increased membrane localization of small-conductance Ca<sup>2+</sup>-activated K<sup>+</sup> (SK)-channels after field stimulation.**

**A**, Representative immunocytochemistry of SK2 in right-atrial (RA)-cardiomyocytes from Ctl-patients after 10 minutes of field stimulation at 0.2 Hz or 5 Hz. Lower panels show transversal line profiles of fluorescence intensity (F.I.). Scale bars indicate 10- $\mu$ m. Bottom panel shows average F.I. of SK2 at the membrane (first and last 10% of cell width) compared to the cytosol (middle 80%) after 10 minutes of field stimulation at 0.2 Hz or 5 Hz. Data are normalized to 0.2 Hz. **B**, Similar to panel A for SK3. **C**, Representative

co-staining of SK2 (red) and  $\alpha$ -actinin2 (green) in RA-cardiomyocytes from Ctl-patients after 10 minutes of field stimulation at 0.2 Hz (left) or 5 Hz (right). Scale bars indicate 20- $\mu$ m. **D**, Pearson's R correlation coefficient for SK2 and  $\alpha$ -actinin2 after 0.2 Hz and 5 Hz pacing. N-numbers indicate numbers of cardiomyocytes/patients. *P*-values are based on multilevel mixed models with log-transformed data (**A**) or regular data (**B,D**) to account for non-independent measurements in multiple cells from individual patients and take into account that cardiomyocytes from the same patients were used for 0.2 Hz and 5 Hz.